TALLINNA TEHNIKAÜLIKOOL
INSENERITEADUSKOND
Elektroenergeetika ja mehhatroonika instituut

RIKKELISTE ELEKTRIMOOTORITE VÄLJATÖÖTAMINE DIAGNOSTIKALABORI KATSESTENDIDELE

DEVELOPMENT OF FAULTY ELECTRICAL MACHINES FOR DIAGNOSTICS LABORATORY TESTBENCHES

MAGISTRITÖÖ

Üliõpilane: Lauri Eensalu

Üliõpilaskood: 144378

Juhendajad: Toomas Vaimann, Vanemteadur
Bilal Asad, Doktorant

Tallinn, 2019

AUTORIDEKLARATSIOON

Olen koostanud lõputöö iseseisvalt.

Lõputöö alusel ei ole varem kutse- või teaduskraadi või inseneridiplomit taotletud. Kõik töö koostamisel kasutatud teiste autorite tööd, olulised seisukohad, kirjandusallikatest ja mujalt pärinevad andmed on viidatud.

"....." ..... 201…..

Autor: .....

/ allkiri /

Töö vastab magistritööle esitatud nõuetele

"....." ..... 201…..

Juhendaja: .....

/ allkiri /

Kaitsmisele lubatud

"....."..... 201… .

Kaitsmiskomisjoni esimees .....

/ nimi ja allkiri /

LÕPUTÖÖ LÜHIKOKKUVÕTE

Autor: Lauri Eensalu *Lõputöö liik:* Magistritöö

Töö pealkiri: Rikkeliste elektrimootorite väljatöötamine diagnostikalabori katsestendidele

Kuupäev: 24.05.2019 69 *lk (lõputöö lehekülgede arv koos lisadega)*

Ülikool: Tallinna Tehnikaülikool

Teaduskond: Inseneriteaduskond

Instituut: Elektroenergeetika ja mehhatroonika instituut

Töö juhendaja(d): Vanemteadur Toomas Vaimann ja doktorant Bilal Asad

Sisu kirjeldus:

Antud lõputöö eesmärgiks on tekitada asünkroonmootorile erinevaid tõrkeid – katkised rootorivardad, mähisevead – ning võrrelda saadud tulemusi terve mootoriga. Täielikult tekitatakse kõik tõrked simulatsioonitarkvara platvormil. Praktilises osas, lõhutakse kolmel rootoril rootorivardad kontrollitud puurimise teel ning teostatakse katselised mõõtmised modifitseeritud elektrimootoritega. Kõik mõõtetulemused salvestatakse ning analüüsitakse antud lõputöös sagedusspektri analüüsi, voolude, momentide või mootori kiiruse muutuse põhjal.

Märksõnad: elektrimasinad, asünkroonmasinad, diagnostika, rikked, seire.

ABSTRACT

Author: Lauri Eensalu *Type of the work:* Master Thesis

Title: Development of Faulty Electrical Machines for Diagnostics Laboratory Testbenches

Date: 24.05.2019 *69 pages (the number of thesis pages including appendices)*

University: Tallinn University of Technology

School: School of Engineering

Department: Department of Electrical Power Engineering and Mechatronics

Supervisor(s) of the thesis: Senior Researcher Toomas Vaimann and Ph.D. student Bilal Asad

Abstract:

The main objective of this thesis is to create various faults in induction machines (broken rotor bars, coil to coil fault, faulty internal coil to coil connection fault) and compare the outcoming results with healthy machine. All of these faults are thoroughly in modelled simulation environment. Practical part experiments are done with broken rotor bars. All the results from the measurements are stored and analysed in this thesis via frequency spectrum, currents, torques, or speeds.

Keywords: induction machines, diagnostics, faults, condition monitoring.

THESIS TASK

Thesis title:	**Development of faulty electrical machines for diagnostics laboratory testbenches**
Student:	**Lauri Eensalu, 144378**
Programme:	**Energy Conversion and Control Systems (AAAM)**
Type of the work:	**Master Thesis**
Supervisors of the thesis:	**Toomas Vaimann and Bilal Asad**
Validity period of the thesis task:	**24.05.2019**
Submission deadline of the thesis:	**24.05.2019**

_____	_____	_____
Student (signature)	Supervisor (signature)	Head of programme (signature)

1. Reasons for choosing the topic

The diagnostics of electrical machines is relevant for every machine manufacturer and user. If enterprise production is entirely relied on electrical machines, then it is vitally important for the process owner to know that in what condition the operating motors are. The diagnostics of the electrical machines enables to get a good overview on the condition of the machine. Based on the results the machine owner can take further actions on maintenance, repair or replacement. The main goal is to prevent any failures or faults suddenly appearing. In this thesis investigation to electrical faults is done through literature studies, simulations and experimental setup.

2. Thesis objective

The main objective of this thesis is to investigate different faults on the electrical machines through simulations and experimental setup that are done in electrical machines laboratory.

3. List of sub-questions:

- Thorough survey to the electrical machine faults
- Modelling of the electrical machine to simulation software
- Valid preparation of the experimental setup

4. Basic data

The stated objectives are intended to be accomplished through literature survey and with studies on the practical electrical machine and simulation software.

5. Research methods

Results are intended to be accomplished with measurements to the experimental machine, literature studies, modelling, and simulating the electrical machine. Data analysis is done with software tools - Excel and Infolytica. Fast Fourier transformation will be applied to gathered data.

6. Graphical material

All together in this thesis there are over fifty figures that are shown throughout the thesis. The most important figures are shown on Paragraphs 3 and 4.

7. Thesis structure

This thesis is divided into 5 chapters and the exact structure can be found on pages 8-9.

8. References

Main source of references are books and scientific journals. Some of the most important references are highlighted below:

1. N. Bianchi, Electrical Machine Analysis Using Finite Elements, Boca Raton: CRC Press, 2005, pp. 21-22,25-26.
2. T. Vaimann, *Diagnostics of Induction Machine Rotor Faults Using Analysis of Stator Signals,* Tallinn: TUT PRESS, 2014, pp. 18,26.
3. A. Hand, Electric Motor Maintenance and Troubleshooting, New York: McGraw-Hill Companies, Inc, 2001, pp. 289-319.
4. B. Asad, T. Vaimann, A. Rassõlkin, A. Kallaste and A. Belahcen, "A Survey of Broken Rotor Bar Fault Diagnostic Methods of Induction Motor," *Scientific Journal of Riga Technical University,* vol. 14, no. 2, pp. 117-124, 2018.
5. G. Bergland, "A Guided Tour of Fast Fourier Transform," *IEEE Spectrum,* vol. 6, pp. 41-52, 1969.

9. Thesis consultants

There are no consultants for this thesis.

10. Work stages and schedule

1. Going through the literature (Deadline: 17.05.2019)
2. Collecting basic data (Deadline: 03.05.2019)
3. Writing theoretical part (Deadline: 17.05.2019)
4. Doing the calculations, measurements, and model (Deadline: 03.05.2019)
5. Describing the results of study (Deadline: 17.05.2019)

6. Writing conclusions (Deadline: 21.05.2019)
7. Completing the first version of the work (Deadline: 21.05.2019)
8. Sending to the supervisor (Deadline: 21.05.2019)
9. Introducing corrections (Deadline: 22.05.2019)
10. Sending to the supervisor for second time (Deadline: 23.05.2019)
11. Final version of the thesis (Deadline: 23.05.2019)

CONTENTS

ABBREVIATIONS AND SYMBOLS

List of Abbreviations

IGBT – Insulated-Gate Bipolar Transistor

SPM – Shock Pulse Measurement

ω – angular velocity

F – force

MCSA – Motor Current Signature Analysis

FEM – Finite Element Analysis

FFT – Fast Fourier Transformation

DTFT – Discrete-time Fourier Transform

STFT – Short-time Fourier Transform

B – magnetic flux density

J – current density

H – magnetic field strength

E – Maxwell's electric field

D – electric displacement

ACKNOWLEDGMENTS

The author is grateful towards Tallinn University of Technology (TalTech) and VSB - Technical University of Ostrava. These universities enable graduates to achieve highly skilful knowledge and experience through Master of Science programs. There would not be new discoveries or highly talented scientists without your support to the students.

The author would like to thank his supervisors Toomas Vaimann and Bilal Asad, and Ants Kallaste, Anton Rassõlkin for assistance. Their contribution has been extremely valuable. Setting objectives, applying right methods and making sure that experiments are done correctly could not have been possible without their supervision and consulting. Moreover, special thanks to all professors, engineers, scientist and researchers who have dedicated their time and effort throughout my Master of Science program.

I would also like to say my deepest and sincerest appreciation to my employer Saksa Automaatika OÜ. Thanks to them I have been able to allocate time plentifully to master's thesis and been able to finish. It would not have been possible without your support. Thank You!

Furthermore, my appreciation goes to Estal Metall OÜ. Thank you for your assistance on electrical motors modification on such a great manner.

Finally, I would like to thank my lovely wife, close family and friends who have motivated me throughout this period. You are the ones who gave me power and strength to move forward, towards my dreams. Thank you a lot!

PREFACE

This thesis has been written in Tallinn University of Technology Department of Electrical Power Engineering and Mechatronics. Simulations, experiments and mechanical modifications were carried out in electrical machines laboratory. Mentor Graphics software Infolytica was used for the simulations. Case study was done with 7.5 kW induction motor, ABB frequency converter and a load motor.

The thesis was proposed by Toomas Vaimann, Ants Kallaste and Anton Rassõlkin. It is in their intention to have a diagnostics laboratory in Tallinn University of Technology, which would enable university students to have a more practical approach into this field. This thesis work is a part of achieving this objective and is a contribution towards this goal.

As such, Master's thesis is divided into five main chapters. At the introduction, an overview is given from the subjects which cover the thesis work. On the second phase, induction motor will be studied for simulation design purposes. After that, on chapters 3 and 4, simulations and experiments will be carried out. In the final part everything is bounded together on conclusion chapter. Information covering electrical drawings, winding configurations, datasheets, etc. are brought out in Appendices.

INTRODUCTION

Induction motors first founders are Galileo Ferraris (1885) and Nikolai Tesla (1886). Since their invention, induction motors are well known and ready for use on industrial scale, since the beginning of 20th of century. However, on a large scale, these motors came widely popular after 1985. Deployment of IGBT technology to PWM inverters made induction motors sensible and practical electrical machines to be used in different type of applications. Abovementioned year marked a significant benchmark for the induction motors [1].

Development and diagnostics of induction motors are thriven by the pressures of growing demands of the industrial market. That is reflected through the increasing population, economic utilization, and lack of resources (copper, mineral material, energy, etc.). Thus, there are major tasks for the electrical motor manufacturers and users on how to reduce energy consumption and prevent any critical failures occurring, which could destroy the electrical machine. Currently, there are no single-handed solutions, which could eliminate all the occurring problems on manufacturing and diagnostics side. Yet, this can be taken as an ideal target. From the practical perspective, it is important for the electrical equipment manufacturers and users to know how the machine is behaving. It would enable all interested parties to take actions based on the information they are gathering and materialize that on designing better electrical machines or applying better preventive maintenance strategies.

In the past, and even nowadays, basic electrical machines diagnostics is mainly done through visual inspection, hearing, touching, and smelling. Based on the gathered information a decision is taken, whether to make maintenance stoppage or not. Unfortunately, that is not a good solution to companies, where electrical machines are located on the critical parts within the process. If they rely to basic diagnostics, then at the end of the day, this company must close its doors. Most competitive companies implement predictive and preventive maintenance programs in their process.

The results of this Master's thesis results are a part of diagnostics laboratory development in Tallinn University of Technology (TalTech). The objective is to guarantee that the graduates at the end of their studies could do diagnostics on practical machines in parallel to the theoretical studies. Furthermore, scientific studies on the electrical motor diagnostics would be possible.

1 INTRODUCTION TO INDUCTION MACHINE AND DIAGNOSTICS

1.1 Three Phase Induction Motor

As shown on Figure 1.1, three phase induction machines typically consist of a terminal box, a stator with windings, bearings, motor shaft, cooling fan, rotor, cooling fins and chassis. Specific design of the motor depends on the application where it is ought to be used. If the motor power dimensions increase, there will be increased need to lubricate the bearings. Typically, in that situation, bearings are constantly monitored through the surveillance of vibration and temperature. Vibration can be measured through Shock Pulse Measurement (SPM) ripples and temperature is monitored through sensors, which are installed in the stator coils [1].

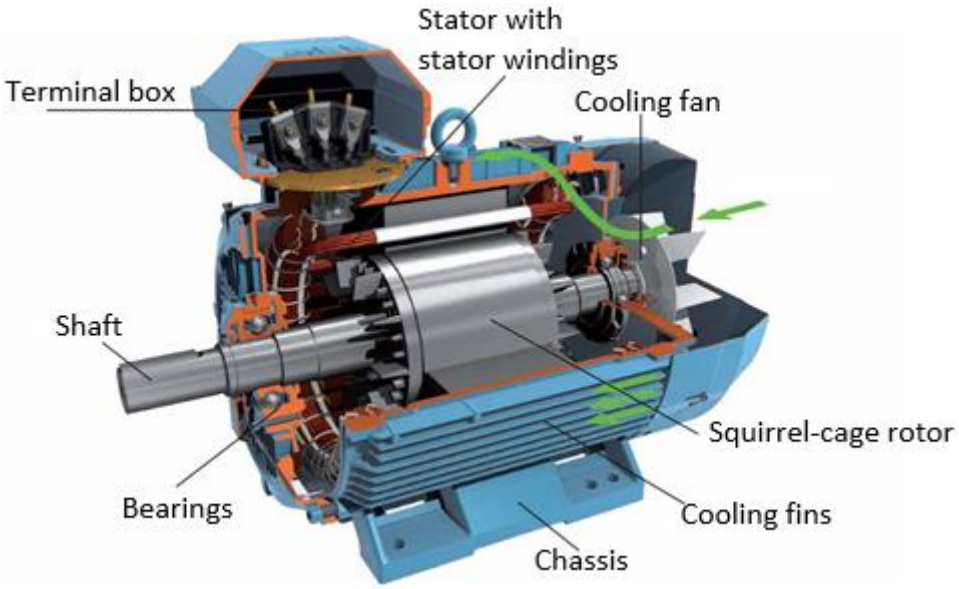

Figure 1.1 Structural design of motor [2]

1.1.1 Rotating Magnetic Field via Stator

Rotating magnetic field is easily generated in the stator with the three-phase alternating current system. Each phase is turned into a coil, which is attached to the stator bores. These coils are installed on the same level of the surface and, compared to each other, they are shifted 120 degrees. Same applies to the electrical current. Every phase current is also shifted by 120 degrees. When alternating current is going through each phase as described in Equation 1.1, then the rotating magnetic field is generated accordingly to Figure 1.2.

$$i_A = I_m \cos \omega t; \qquad i_B = I_m \cos\left(\omega t - \frac{2}{3}\pi\right); \qquad i_C = I_m \cos\left(\omega t + \frac{2}{3}\pi\right) \tag{1.1}$$

Where i_A, i_B, i_C are the stator currents, I_m is the current modulus, ω is the angular velocity (rad/s), t is the time [3].

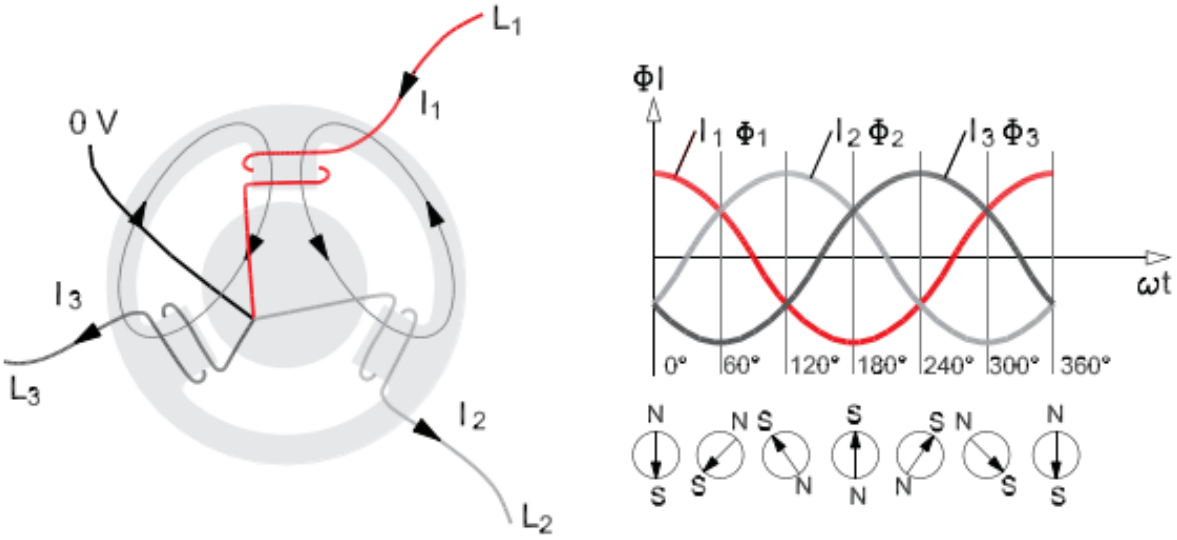

Figure 1.2. Rotating magnetic field on 1 pole pair electrical machine [4]

Rotational speed of the magnetic field is dependent on the number of pole pairs in stator:

$$f = \frac{pn}{60} \rightarrow n = \frac{60f}{p} = \frac{60 \cdot 50}{p} = \frac{3000}{p} \tag{1.2}$$

Where *f* is the frequency of the grid (50 Hz), *n* is the rotations per minute (rpm), p number of stator pole pairs.

Accordingly, to the Equation 1.2 and Figure 1.2, the rotational speed of the magnetic field would be 3000 rpm. On a four pole pair machine it would be 750 rpm [5].

1.1.2 Axial Current Flow through the Rotor

The rotor is a rotational part of the induction machine, which is fixed to the motor with bearing housings. There are two main types of rotors used on induction machines. One of them is the squirrel-cage rotor (Figure 1.3, a) and the second one is the wound rotor (Figure 1.3, b).

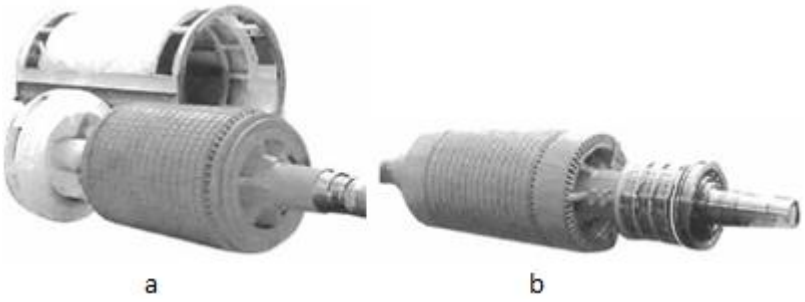

Figure 1.3. a - squirrel-cage rotor; b - wound rotor [6]

In practice, the squirrel-cage rotor is most widely used, as it has the least aging components and is simpler on its design. The main drawback of the induction motor are the bearings, which under normal circumstances have the shortest lifetime due to wearing. Yet, on a small-scale motor they are usually designed to last for a lifetime.

Squirrel-cage rotor is typically made from axially laminated steel plates, which are pressed together or attached to rotor shaft in a manner that they are fixed. After fixation, laminated plates are casted in a mould, where the slots and openings are filled with molten aluminium or copper. Thereafter, rotor bars, end rings and ventilating ends are formed (Figure 1.4) [5].

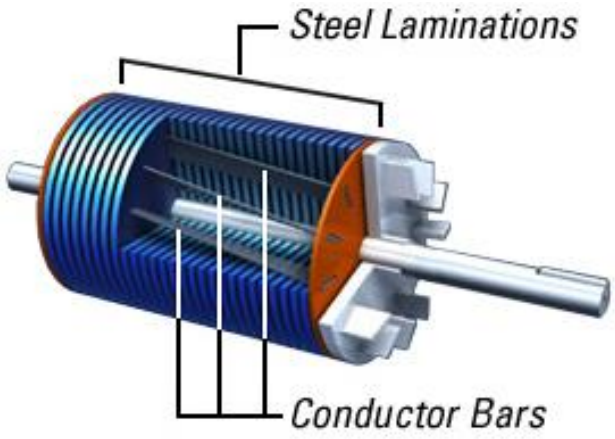

Figure 1.4. Squirrel-cage rotor structural view [7]

End rings connect the rotor bars to each other, and shorted circuit is formed. When such a circuit is placed in fluctuating magnetic field, current I_w will be induced in rotor bar and electromagnetic force is generated. As shown on Figure 1.5, that force causes the rotor to rotate [4].

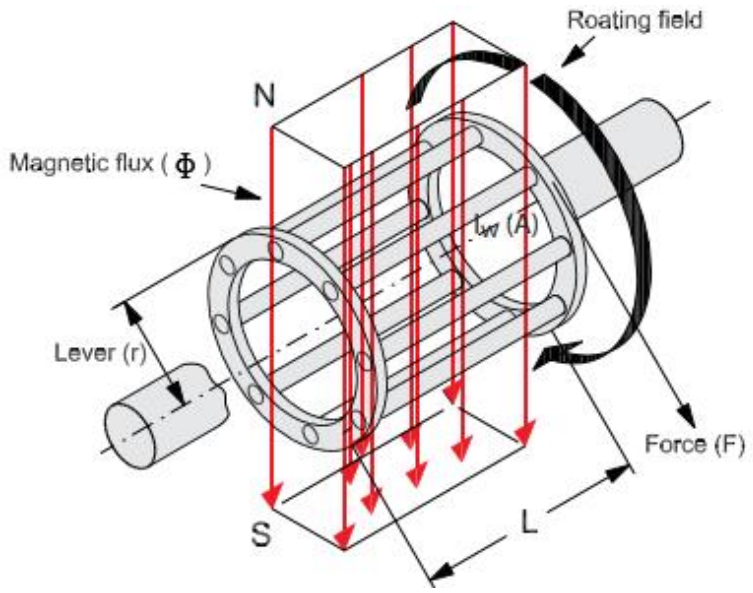

Figure 1.5. Operational field and squirrel-cage rotor [4]

When the angle between force *F* and magnetic flux density *B* is 90 degrees, the applicable force to the rotor is

$$F = B \cdot I_w \cdot L, \tag{1.3}$$

where *L* is the length of the rotor bar.

Likewise, the main vectors that describe the electric and magnetic fields are the magnetic flux density **B**(P,t), current density **J**(P,t), magnetic field strength **H**(P,t), Maxwell's electric field **E**(P,t), and electric displacement **D**(P,t). *P* marks the location of the vector and *t* is time [8].

Furthermore, these vectors have interrelation to each other through the Maxwell's Equations:

$$curl\boldsymbol{H}(P,t) = \boldsymbol{J}(P,t) + \frac{\partial \boldsymbol{D}(P,t)}{\partial t} \tag{1.4}$$

$$curl\boldsymbol{E}(P,t) = -\frac{\partial \boldsymbol{B}(P,t)}{\partial t} \tag{1.5}$$

$$div\boldsymbol{B}(P,t) = 0 \tag{1.6}$$

$$div\boldsymbol{D}(P,t) = \rho(P,t) \tag{1.7}$$

Where, ρ is the volume density of free charge [8].

1.2 Faults in Electrical Machines

Maintaining the electrical machine running with maximum utilization is not an easy target for the companies and machine users. Achieving this goal requires extensive knowledge of the application and environment, skilful staff and right priorities. On the reverse, it is common that electrical machines fail because of improper or no maintenance, invalid machine selection for the application, bad handling (cyclic operation e.g.), overloading, harsh environment, unbalanced voltage, etc. As an outcome, electrical machine may have mechanical failures, electrical breakdown, or both at the same time. Based on their severity, these faults can lead to the requirement of replacing or rewinding of the motor. All of that can be avoided if the first assessment of the application is done properly and maintenance is prioritised.

Based on a large survey carried out by IEEE and shown on Figure 1.6, bearing faults form 41% of all the faults in electrical machines. 37% are related to stator faults, 10% are rotor related faults and remaining 12% of faults cannot be classified [9].

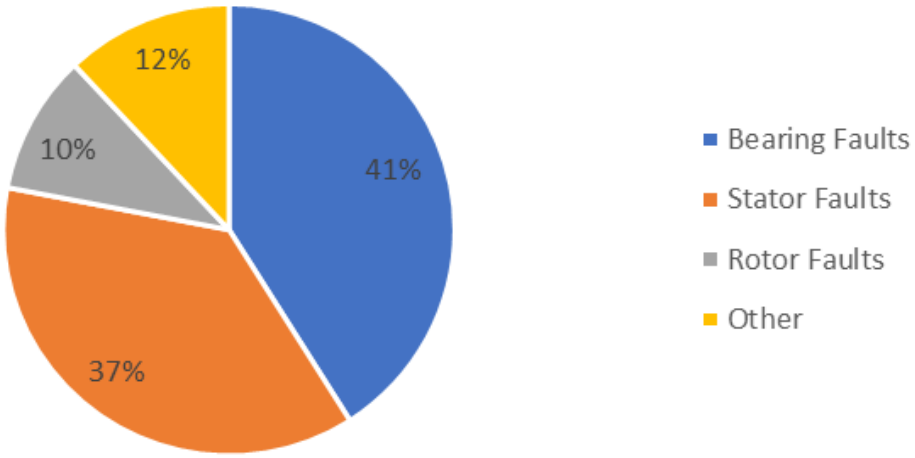

Figure 1.6. Statistical outcome of IEEE survey

1.2.1 Stator Winding Failures

Out from 37% of stator faults, the most common failures are brought out on Figure 1.7. Severe failures, such as phase-to-phase failure, begin with one of the smaller failures as follows - excessive coil movement, aging of the insulation, hot spots, nicked coil wire, high-voltage spikes as on Figure 1.8, overvoltage, undervoltage, wrong supply frequency, overheated windings, and loose, vibrating coil wires. These problems can be avoided with proper safety regulations, handling and through improved assembly of the machine in production or repair process [10].

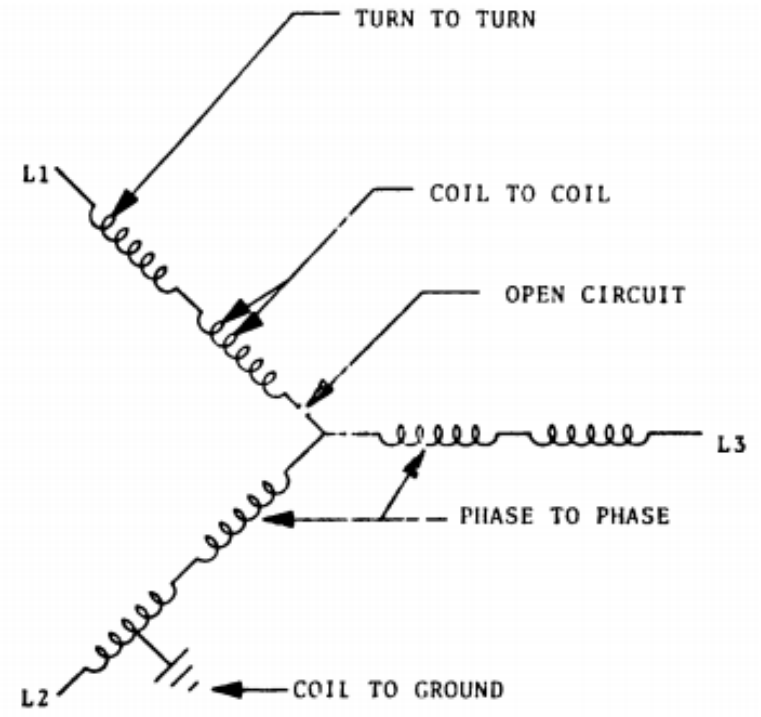

Figure 1.7. Stator winding faults [11]

Turn to turn failure is one of the most common failures in the stator winding. In this situation, usually one or more turns of a coil are bypassed, and closed-loop circuit is formed. Thereafter, this closed-loop circuit is cut by the lines of force (from ac current flow) and high current flow will appear in the phase. Rising current will cause the closed-loop circuit to melt open again, which in turn will cause ampere demand to decrease and the consumption will be close to equal to the normal phases. This kind of fault is easily detectable on the electrical motor. High consumption of the current in one phase will be detected or visually it can be seen when the windings get charred. On top of that its magnetism causes a ringing sound, which is unique to shorted turns. In stall position, the fault can be detected through the phase resistance measurement. There is a small difference in resistance between faulty and normal phases. Coil to coil fault in principle is similar to turn failure [10].

A step further and more severe fault is the phase to phase fault. In this case a large amount of winding is bypassed, which will cause both phases to melt open. Typically, it happens within the stator slots, and copper is fused to the slot laminations [10].

Open circuit fault will increase the current flow in two phases. As a result, these phase windings will overheat and char. This fault can suddenly appear, if there is any failure such as phase-to-phase short, shorted turns, faulty internal coil-to-coil connection, etc [11].

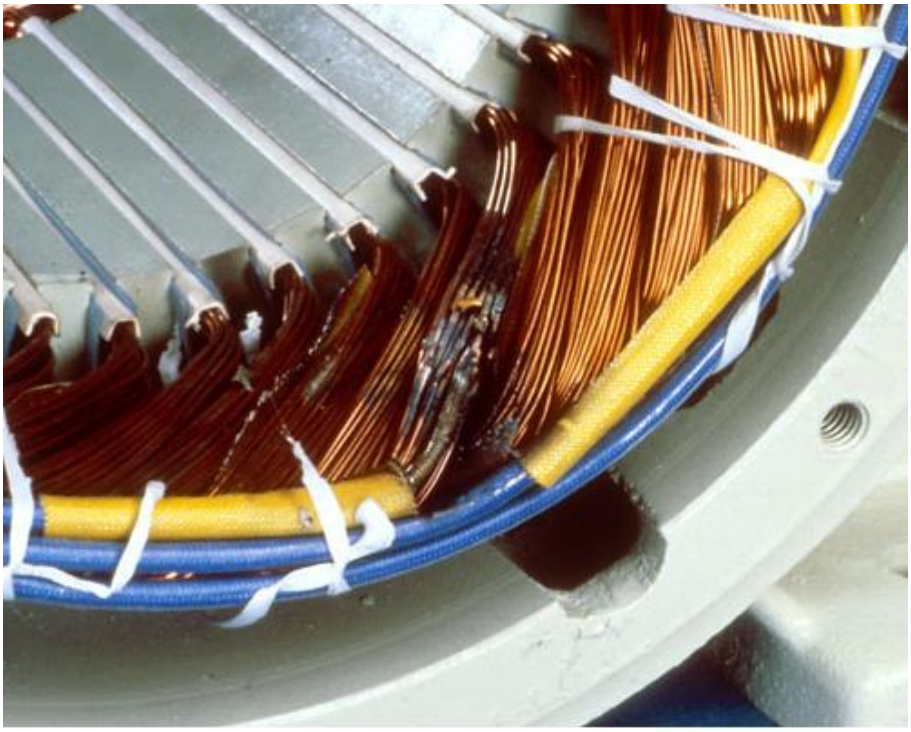

Figure 1.8 Winding damage caused by the voltage surge [12]

1.2.2 Rotor Faults

Accordingly, to paragraph 1.2.2, induction motor rotor is made from steel laminations, which are casted into aluminium or copper to form squirrel-cage rotor. Although its structure looks strong and solid, rotor faults are still relevant to electrical machine users.

These faults are mainly caused by thermal, magnetic, residual, mechanical, dynamic, and environmental stresses. In each of these categories there is a wide spectrum of different failures and out from these failures a brief outline of rotor problems is shown on Figure 1.9 [13].

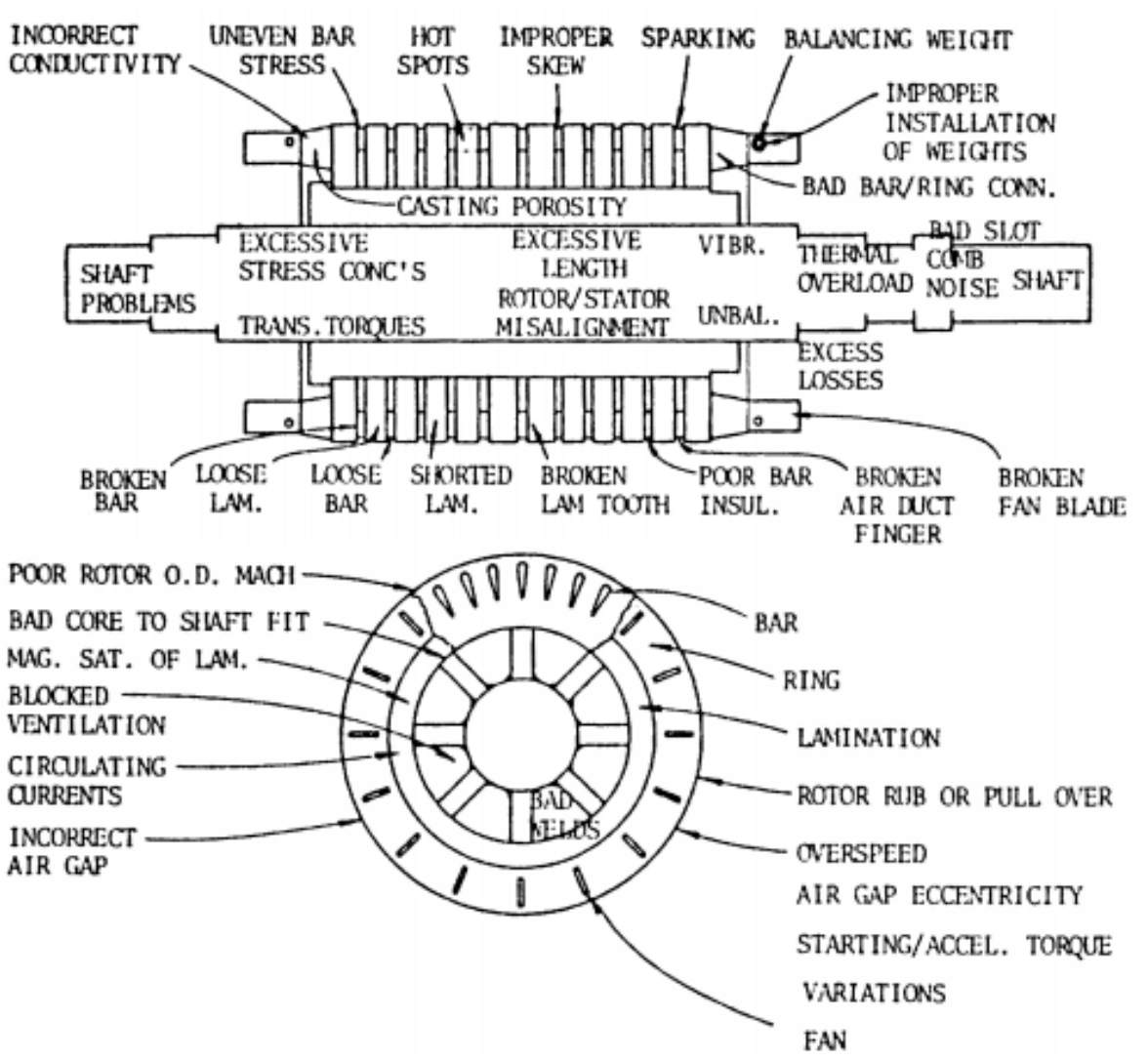

Figure 1.9. Rotor schematic and possible causes of the faults [13]

Broken Rotor Bars

On a squirrel-cage motor, a broken rotor bar is typically caused by the excessive forces of the stator electromagnetic field. The rotating field will cause rotor to rotate and on the other hand can cause

a rotor bar to break, crack or separate from the end ring. At the early stage, if no damage is done to the stator, then this fault is hardly detectable. Yet, it has an imminent effect on the healthy bars, which are next to the broken bar or bars. Current flow in rotor becomes disproportionate and will lead to increased rms value of current and temperature in healthy rotor bars. This abnormal condition can have a cascading effect, so that the rotor becomes completely malfunctioning [9], [14].

1.2.3 Other Electrical Motor Faults

Other electrical faults which could occur in motor are related to the loading of the machine, improper supply, bearings, bad handling.

Overvoltage, unbalanced voltage and low voltage with nominal load commonly have similar effect to the electrical motor. In short time, the machines start to overheat during motor operation. Overheating will lead to insulation breakdown and the motor will short circuit or char itself. It is possible to run the motor with deviated values, but NEMA standard must be kept in mind. It allows the motors voltage deviation of $\pm$ 10% percent. As an example, unbalanced voltages cause the motor to have uneven magnetic field distribution between poles and that will lead to generation of harmful harmonics. If such operation continues, motor will have final condition as shown on Figure 1.10. One phase gets charred, second one is discoloured, and third phase will look fine [10].

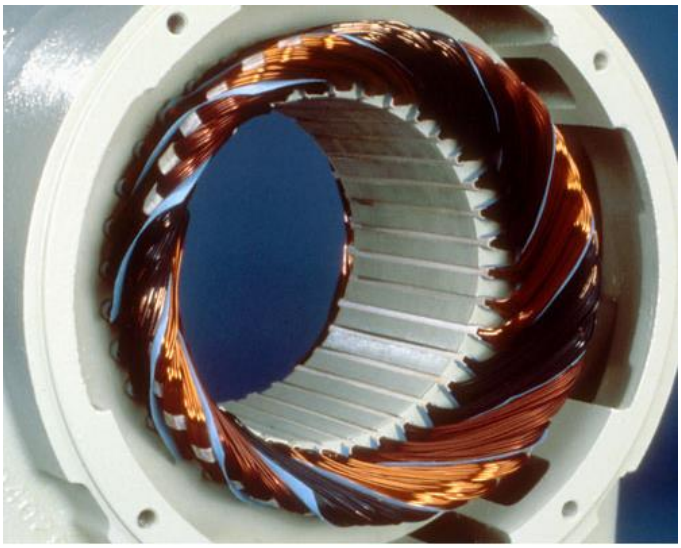

Figure 1.10. Damage caused by unbalanced voltage [12]

As Figure 1.6 emphasizes, bearing failures contribute 41% to all failures in the electrical machines. These failures may be caused by improper lubrication, contamination, mechanical wear, corrosion, improper handling, tilted shaft, etc. On Figure 1.11 some bearing failures are brought out. Bearing failure becomes imminent when the rotor starts dragging the stator [10], [15], [16]. These faults can be detected on a very early stage, when vibration and temperature monitoring is done on bearing housing. Bearings analysis and cause of faults is thoroughly described in paper [16].

Finally, the bad handling of the electrical machine can cause the breakdown of the machine. As usual, overheating of the machine is caused. If machine user is paid by the volumes of units, which the machine can push through the system, then the overloading of the machine can get relevant. In addition to that, frequent start-stop operations and abrupt speed changes are harmful to all motors. Thus, the machine operator must know precisely the application of the motor and choose out relevant type and size of the machine [10].

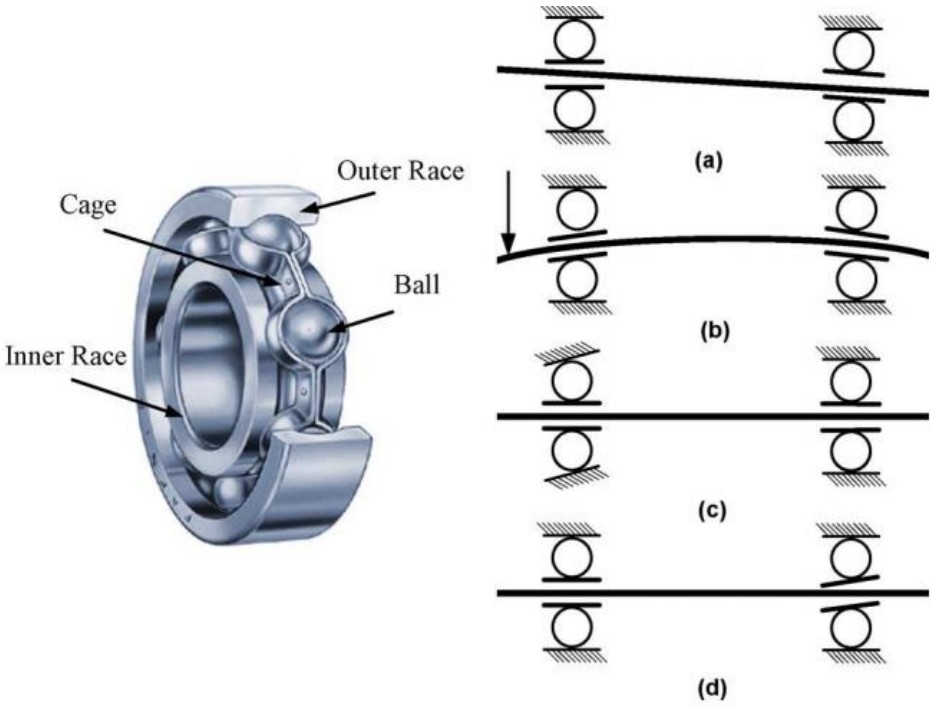

Figure 1.11. Failures of the bearing – (a) misalignment (b) tilted shaft (c) outer race tilted (d) inner race tilted [15]

1.3 Diagnostic Methods

In [17] and on Table 1, journal paper authors highlight that the most common faults are related to mechanics, electricals and environment. Electrical faults are mostly related to the stator and are commonly diagnosed through relays and switches, or with MCSA (Motor Current Signature Analysis) diagnostic methods. Mechanical faults are mostly related to the rotor and are detected through mechanical vibration monitoring, MCSA and FEM (Finite Element Analysis). Environmental failures are addressed to both and can be detected via installed sensors or through protective devices [17].

Besides MCSA, FEM and mechanical vibration monitoring there are several assisting techniques, which are used in fault detection. With a focus on broken rotor bars, following assisting techniques are used - FFT (Fast Fourier Transformation), DTFT (Discrete-time Fourier Transform), STFT (Short-time Fourier Transform), FPGA (Field-programmable Gate Array), fuzzy logic, notch, Gabor transform, Hilbert transform, Wavelet, analytical, Time frequency analysis, etc. Ultimately, these assisting techniques have various pros and cons between each other. Depending on the specific application and technical background, choosing out the best combination for diagnostics can be rather difficult. For example, if the technique called „slot harmonics“ [17] together with MCSA and FFT is used, then compared to technique called „adoptive notch filter“ there is a trade-off between simplicity and accuracy of the system. „Adoptive notch filter“ requires a lot less mathematical calculations and PC memory, but on the other hand its operational area is more limited [17].

Table 1. Most common faults, types and their diagnostic methods [17]

Sr. No.	Category	Types	Location of the faults	Common diagnostic methods
1	Electrical	• Unbalanced supply voltage • Over or undervoltage • Phase reversal • Inter-turn short circuit fault • Earth fault	Mainly stator	• Relays & switches
2	Mechanical	• Broken rotor bar • Broken end ring • Eccentricity fault • Bearing fault • Rotor winding failure	Mainly rotor	• Mechanical vibration detection • MCSA • Finite Element Analysis
3	Environmental	• Ambient temperature • External moisture • Vibration due to bad foundation, etc.	Both	• Sensors and protective devices

1.3.1 Fast Fourier Transformation

Fourier transformations are used for describing linear systems and continuous waveforms. When these transformations are applied to continuous waveforms, the frequency components become visible. In practice, when the waveform is going to be analysed, discrete Fourier transformation (DFT) is used. DFT is the finite version of the Fourier transformation. Successively, fast Fourier transformation is just an effective method for obtaining discrete Fourier transformation (DFT) results [18].

Fourier transform pair for continuous signals are described by the Equations (1.8) and (1.9):

$$X(f) = \int_{-\infty}^{\infty} x(t) e^{-i2\pi ft} dt \tag{1.8}$$

$$x(t) = \int_{-\infty}^{\infty} X(f) e^{i2\pi ft} dt \tag{1.9}$$

Where, $-\infty < f < \infty$, $-\infty < t < \infty$, and $i = \sqrt{-1}$, $X(f)$ is the frequency-domain function, and $x(t)$ is the time-domain function.

Accordingly, if the sampled version is analysed, DFT Equations (1.10) and (1.11) are applied:

$$X(j) = \frac{1}{N} \sum_{k=0}^{N-1} x(k) e^{-i2\pi jk/N} \tag{1.10}$$

$$x(k) = \sum_{k=0}^{N-1} X(j) e^{i2\pi jk/N} \tag{1.11}$$

Where, $j = 0,1, \dots, N-1$; $k = 0,1, \dots, N-1$; $X(j)$ and $x(k)$ are complex series [18].

Real signal and its corresponding DFT in FFT algorithm format are shown on Figure 1.12. On that figure $x(k\Delta T)$ is the time series and ought to be periodic throughout the time domain of period *T* seconds. In accordance to that set of Fourier coefficients $X(jf_0)$ is expected to stay the same during sample period f_s. This is in a more detailed way written out in paper [18]. From calculation operations perspective comparison is brought on Figure 1.13. It clearly shows the advantage of FFT over direct calculation of DFT.

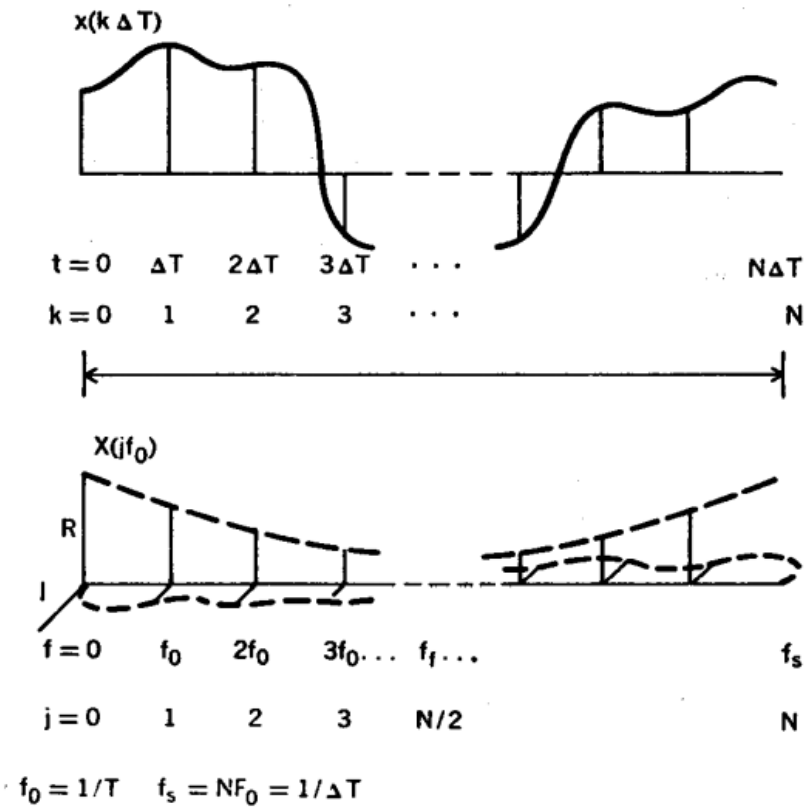

Figure 1.12. Real signal (top) and FFT output of computed signal (bottom) [18]

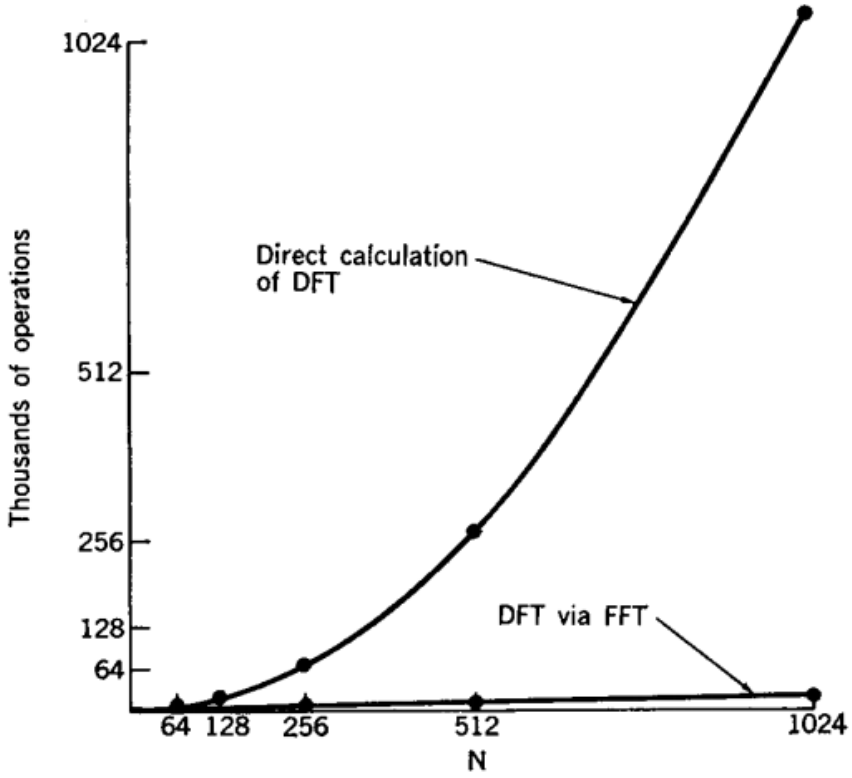

Figure 1.13. Number of operations required with and without FFT [18]

1.4 Modelling Techniques in Fault Diagnostics

Fault diagnosis modelling methods are categorised into three different groups. Previously mentioned FEM is a part of model-based category, MCSA is a part of signal processing techniques and fuzzy logic, artificial neural network, etc. are a part of soft computing technique [19].

1.4.1 Finite Elements Method

Finite elements method is used in fault diagnostics when the accurate model of the faulty machine is well-known. The machine analyser must know precise information on used materials, geometry, environment, etc. When the machine design is ready, numerical technique is applied for computing electric and magnetic fields. Essentially, FEM uses numerical technique based on Maxwell's Equations. Thus, it enables to analyse the electrical machine fields in every structure together with time-variable fields, materials that are anisotropic, non-linear or non-homogeneous. This method is known since 1940s and is most widely used method for the solution of vector field problems [8].

On Figure 1.14 two-dimensional design of electrical motor with mesh elements is shown. Mesh elements are the segments from the domain, which are calculated to hold numerical values of electric and magnetic fields. Mesh in two-dimensional problems is usually formed with triangular or rectangular elements [8]. Electrical machine model below is based on the actual electrical motor. It has been designed with all the right dimensions, materials and attributes.

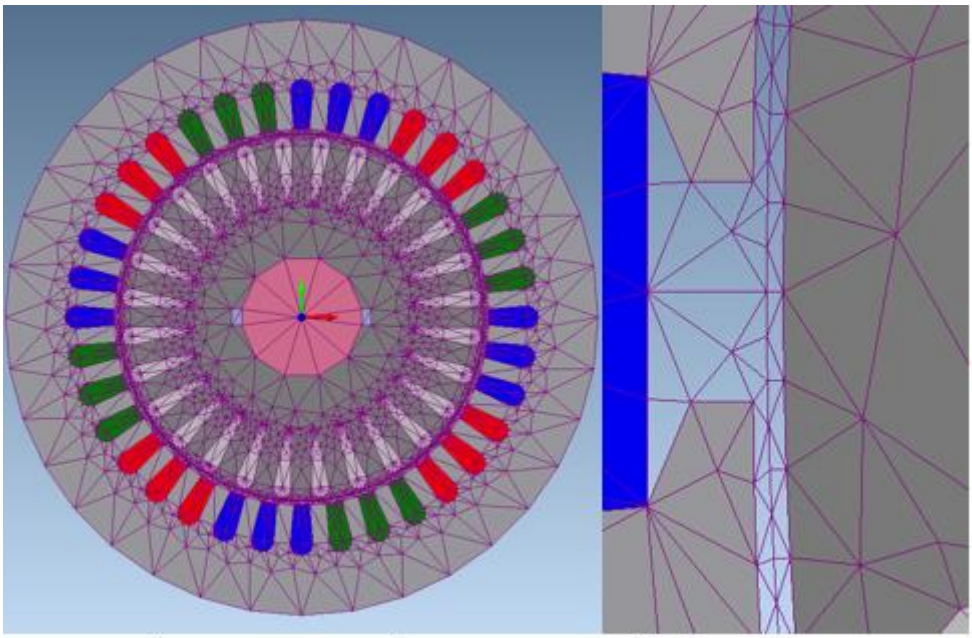

Figure 1.14. Finite elements electrical motor model with mesh elements

It is necessary to define attributes (material, conductivity, motion, boundaries, electrical circuits, etc.) to all objects – rotor shaft, laminations, rotor bars, air gap, stator slots, etc. - as mesh values are significantly affected by these variables. Mesh size gets denser when different materials border each other - [8] e.g. on Figure 10 b, a close view of the air gap is shown. It is known for every machine manufacturer that air gap significantly affects machine behaviour. As such, we can also see that the mesh size defined in that area must be very small in order to get as precise as possible electric and magnetic field values.

1.4.2 Motor Current Signature Analysis

As highlighted in Paragraph 1.3, there is a wide variety of faults, which occur in electrical machines. Most of the faults leave a mark to machines operational behaviour and generate distortions in the supply line of the motor. Motor current signature analysis (MCSA) is the most well-known fault diagnosis method. While motor operates on a steady-state mode, its demanded current from the grid is analysed. The main objective of this method is to evaluate the amplitudes of different harmonics [20]. Thus, it enables to do evaluation on motors current condition and therefore it is a good method on preventing any critical failures and detect them at an early stage. Accordingly, [21] following faults can be detected:

- Broken rotor bars,
- Stator winding problems (short circuit),
- Mechanical problems,
- Abnormal levels of air gap eccentricity.

As an illustration, rotor damages (broken bars and end ring faults) are described by Equations (1.12) and (1.13). Equation (1.12), is used to find the sideband components of the first harmonic. This is typical for the broken rotor bars. Secondly, in order to ratify the presence of rotor fault, Equation (1.13) is used to see whether sideband components exist near the fifth harmonic, when $k/p = 5$. In case of healthy motor, these sideband harmonics will not appear.

$$f_{bb1} = [1 \pm 2ks] \cdot f \tag{1.12}$$

$$f_{bb2} = \left[\frac{k}{p}(1-s) \pm s\right] \cdot f \tag{1.13}$$

Where, s is slip of the rotor, f frequency of the supply, p pole pair number and $k = 1,2,3 \ldots$ [20].

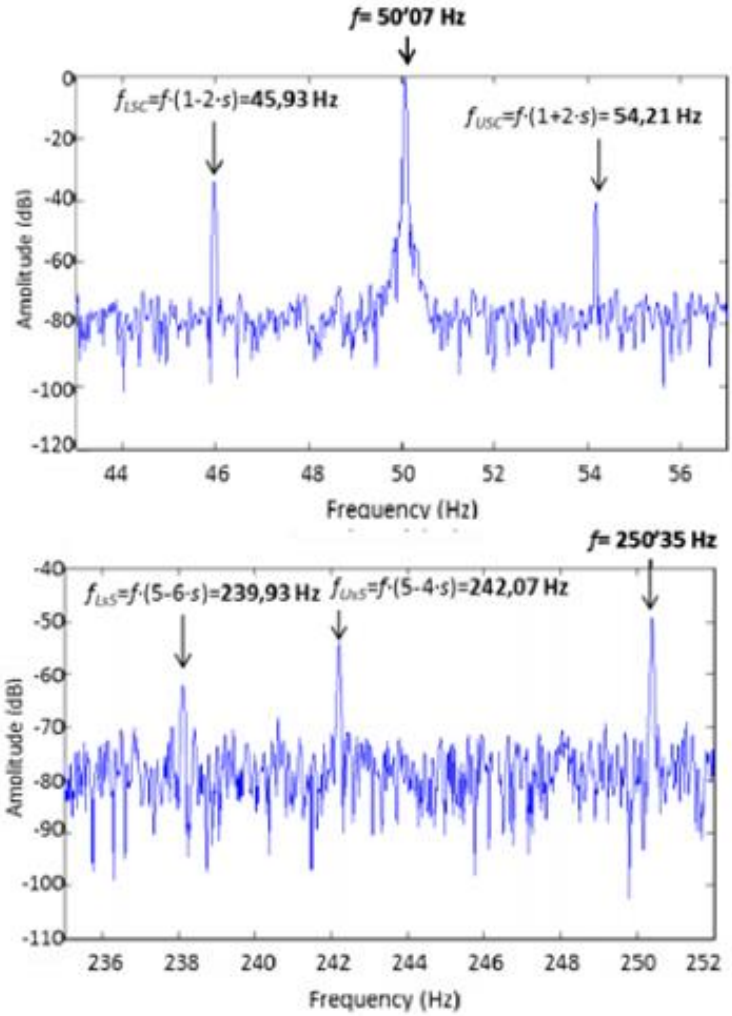

Figure 1.15. Current spectrum in case of two broken motor bars [20]

Furthermore, Figure 1.15 shows the appearance of sideband components (top) and fault components (bottom) near the fifth harmonic. This is relevant pattern for the broken rotor bars [20].

Although rotor bar faults have a quite recognizable pattern, with eccentricity it is quite the opposite. From the literature it is known that static and dynamic eccentricity exist. In practice, none of those exist individually. There is no unique threshold level, which could be applied to the MCSA monitoring. The best way to deal and detect eccentricity problems through MCSA is to monitor the amplitude levels of different harmonics in the stator current spectrum. Equations (1.14) and (1.15) are universally accepted for evaluation, whether the eccentricity fault exists in a machine or not [16].

$$f_{ecc1} = \left[1 \pm m \cdot \left(\frac{1-s}{p}\right)\right] \cdot f \quad (1.14)$$

$$f_{ecc2} = \left[(k \cdot R \pm n_d) \cdot \left(\frac{1-s}{p}\right) \pm n_w\right] \cdot f \quad (1.15)$$

Where, s is slip of the rotor, R number of rotor slots, $m = 1,2,3 \dots$, $n_d = 0$ for static eccentricity and 1 for dynamic eccentricity, f frequency of the supply, p pole pair number and $k = 1,2,3 \dots$. [20]

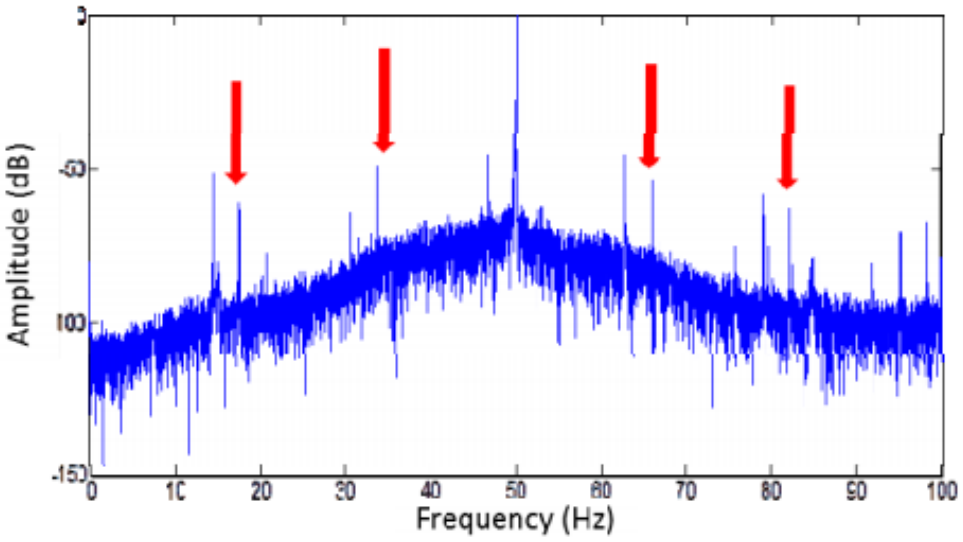

Figure 1.16. Occurrence of eccentricity (Red arrows highlighting high amplitude harmonics) [20]

1.4.3 Soft Computing Techniques

Soft computing technique has gained a lot of interest in recent decades. Its primary reason is that it resembles the human mind, learning in chaotic environment. The techniques of artificial neural network, fuzzy logic, adaptive neural fuzzy inference system, genetic algorithm improve the diagnostics process. Data is interpreted more precisely and arising problems become more manageable (e.g. automatic notification from the system) [19].

In practice, the acquired data from the field machine is pre-treated and so-called intelligent data is sent to the soft computing technique loop. Thereafter, this loop will determine, whether a certain failure exists in the motor or not. This is structural approach is also shown on Figure 1.17.

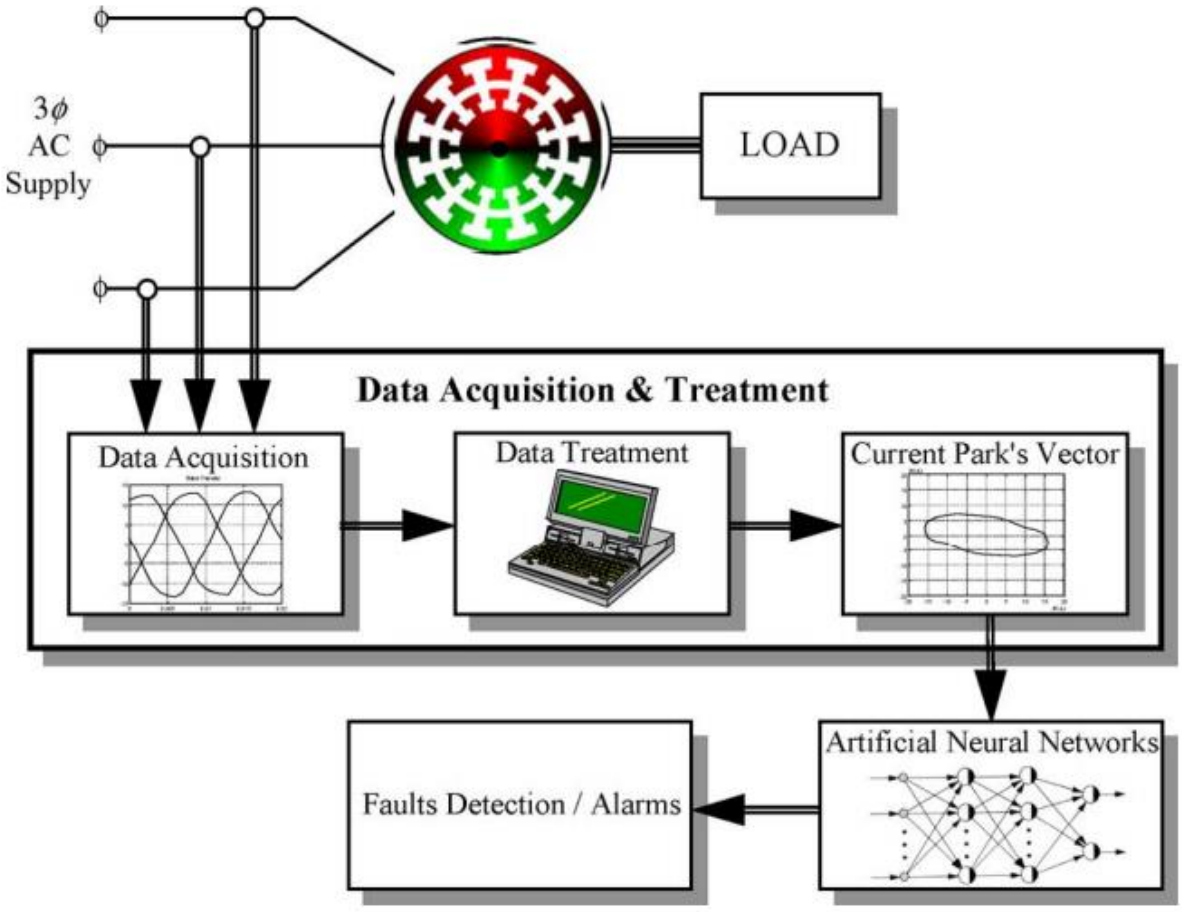

Figure 1.17. Induction motor field data analysed by the artificial neural network [15]

1.5 Aim of the Study

The aim of the study of this thesis work is to design two-dimensional induction motors based on the actual ones and analyse them by using finite elements. Several cases of induction motors will be analysed – healthy and faulty. The main goal is to achieve very precise simulation results and plot current envelopes, currents behaviour in rotor, spectrum analysis of current and speed graphs. These graphs should highlight that the motors' behaviours have significantly changed. Subsequentially, actual motors should replicate closely the simulation results – specific patterns, values, etc.

2 CASE STUDY OF INDUCTION MACHINE UNDER EXAMINATION

2.1 Geometry and Winding Configurations

2.1.1 Rotor Attributes

Examined rotor is made from steel laminations, which are stacked together. It has been casted into molten aluminium mould, which creates rotor bars, end rings and cooling blades. Skewed rotor bars are short-circuited through aluminium end rings. Complete assembly is shown on Figure 2.1.

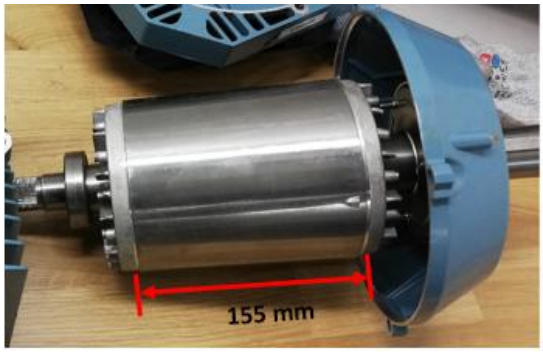

Figure 2.1. Healthy motor rotor

On Figure 2.2 the cross-sectional view of the rotor is shown. As it can be seen, the rotor diameter is 135 mm and shaft is 45 mm. Rotor bars are 155 mm in effective length, 25.40 mm on height, and have varying width of 2 - 6.75 mm. More detailed information is brought out in Appendix 2.

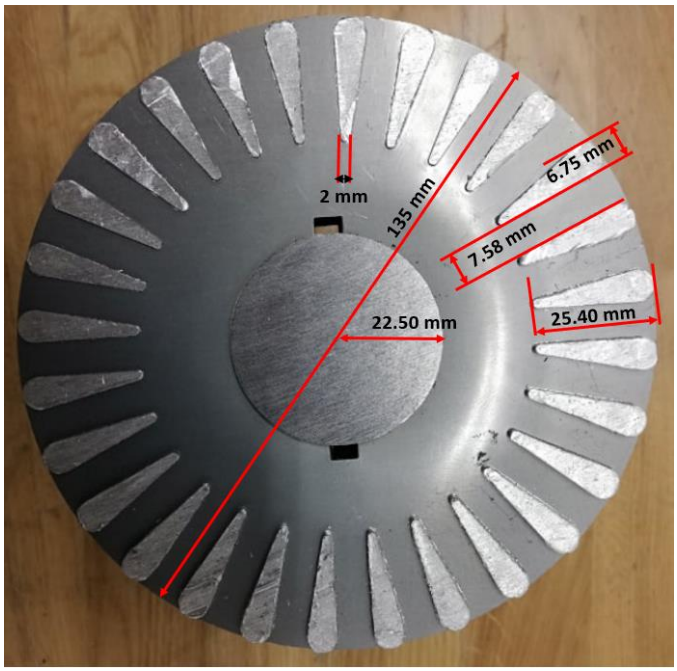

Figure 2.2. Cross sectional view of the rotor

2.1.2 Stator Attributes

As shown on Figure 2.3, the stator is made of steel laminations, which are stacked together. Four copper wires that run in parallel are turned into a coil that has 36 turns. Altogether there are six coils in series per phase and it is a four-pole machine, with 36 stator slots.

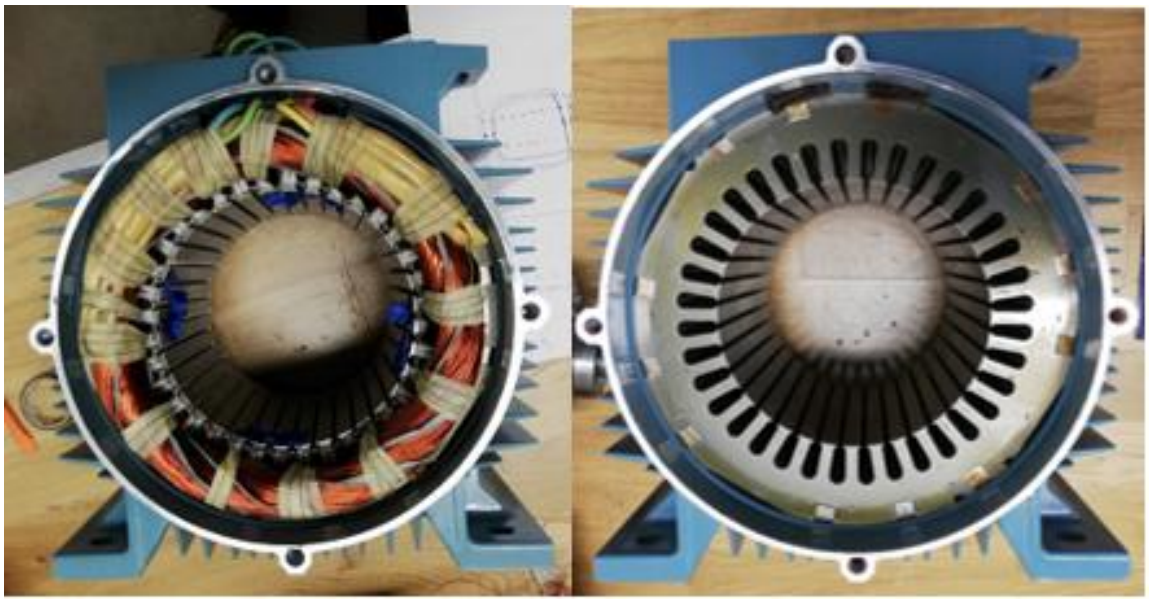

Figure 2.3. Healthy motor stator - wound (left) and without windings (right)

Figure 2.4 shows the stator winding configuration. This winding configuration is not typical as it has a slot pitch variation of 7 and 8. On the four coils, which are turned on the same direction, stator has a slot pitch of 8 and two coils, which have the opposite turn direction has slot pitch of 7. On the supply terminal box, it is also highlighted that these motors are ought to be run with frequency converters. More detailed information from the stator is shown on the datasheet in Appendix 2.

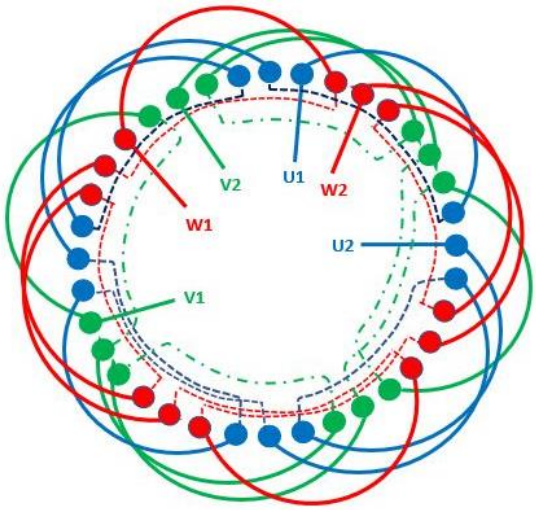

Figure 2.4. Stator winding configuration

3 SIMULATION OF INDUCTION MACHINE

3.1 Setup

Simulation is done based on the actual induction machine design, which does not mean that it is the exact replica. All the dimensions and attributes of the machine are considered to extent which are known for the author. There are several important remarks that are necessary to highlight before the actual simulation results:

1. No skewing effect of the rotor is considered.
2. It is a two-dimensional machine. Hence, the end rings are left out and interconnection of the rotor bars is made through the electrical circuit (Figure 3.1).
3. Machine effective length is 155 millimetres.
4. Current source is considered ideal for the circuits.
5. All the motor connections are done in star connection.
6. Applied load throughout the simulations is constant - value of 49 Nm
7. Simulations on the 900 ms graphs are done with recording frequency of 25 kHz and 1800 ms graphs are done with 1 kHz data recording time. Simulation time with time-series of 900ms is about 36 hours.
8. Stator winding used in simulation is shown on Figure 3.2

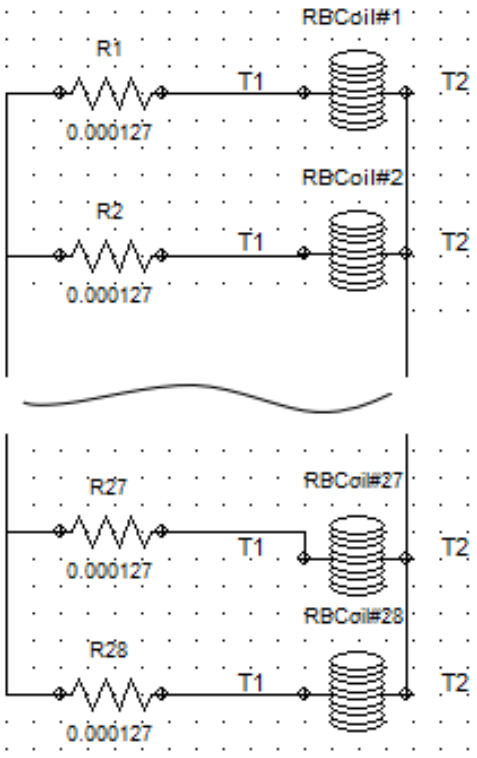

Figure 3.1. Rotor bars connection diagram

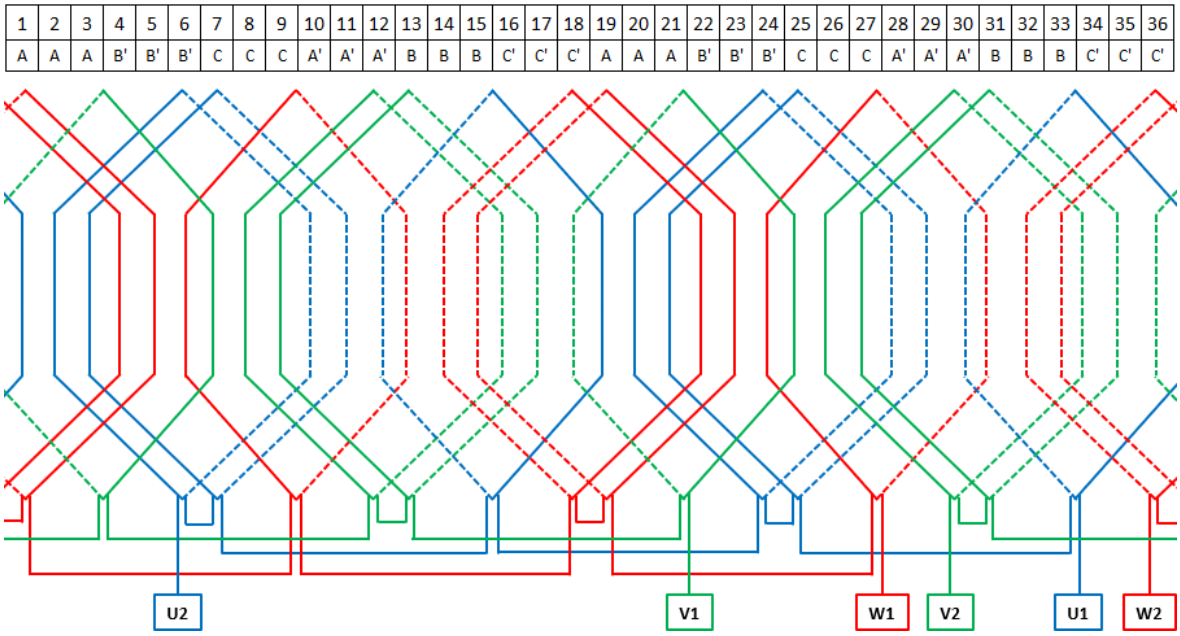

Figure 3.2. Stator winding diagram

Circuit drawings for healthy motor, three broken bars, coil to coil fault and faulty internal coil to coil connection are brought out in Appendix 3. One and two broken bars faults are similar to three broken bars, so there are no circuit diagrams for these. In case of three broken bars, bars number 5, 6 and 7 are faulty, in case of two broken bars these are 6 and 7, and in case of the one broken fault, it is only the 7^{th} bar.

In these connection diagrams there are 28 rotor bar coils and 36 stator coils with 3 current sources. Rotor bar coil consists of small added resistance and material used is aluminium. Stator coils are stranded wires and from copper material. When the coil is stranded, the number of turns and specific resistance value must be calculated and inserted to properties window. Other forthcoming values are calculated by the FEM software.

3.2 Simulation Results of Induction Machine

3.2.1 Healthy Motor and Broken Bars

On Figure 3.3, the induction motor has reached its full saturation. All the four poles of the machine are visible and magnetic distribution between the poles is in good correlation. There are no significant variations between the poles.

On Figure 3.10, the current envelope of healthy motor has a very slight fluctuation, and in addition to that, on Figure 3.11, the speed has a no ripples at all in steady state condition. All of that indicates that the machine is running in normal healthy condition.

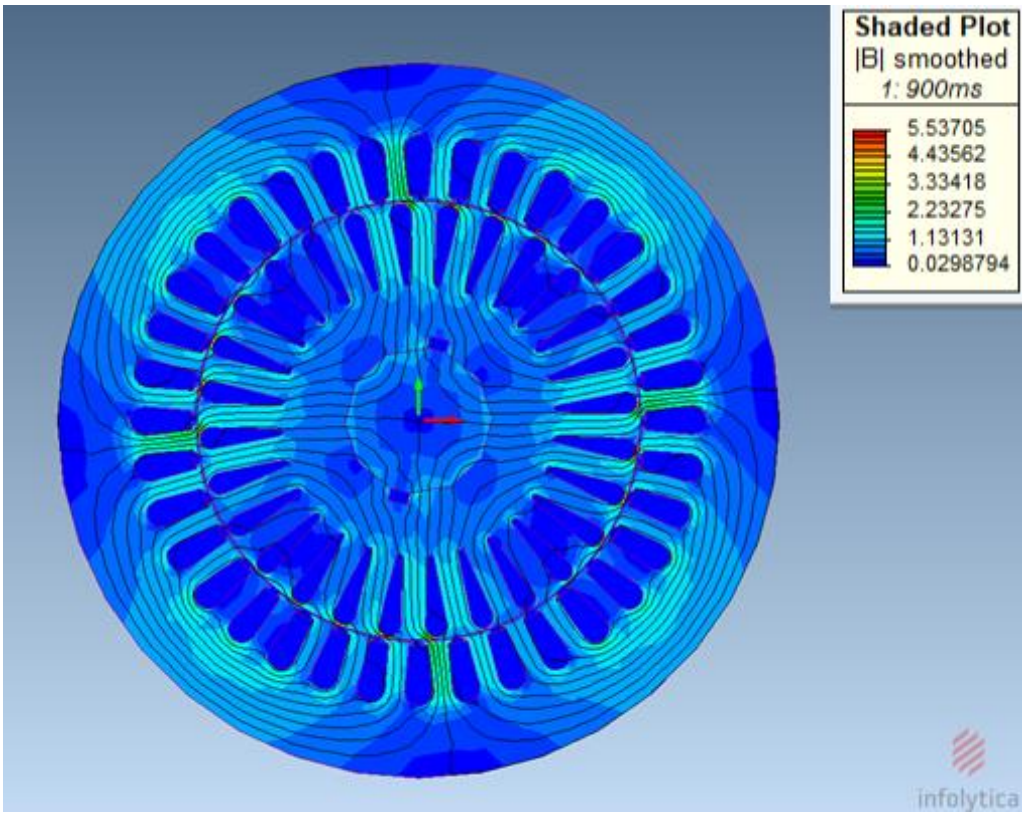

Figure 3.3. Magnetic field distribution of a healthy motor at steady state

The next motor is shown on Figure 3.4 and it has one broken bar fault (marked with red). When looking at the magnetic distribution inside the motor, it looks all fine. Yet, when taking a closer look to rotor bar number 7, its neighbouring bars (6, 8), and comparing these against the opposite bars, there is a slight difference detectable in magnetic field distribution. Current distribution on Figure 3.5 shows clearly that there has been a significant change in rotor bar currents. The siding bars have higher currents than the opposite bars and when comparing the healthy machine to the faulty machine, it can be seen that the signal is not matching up at all. From Figure 3.10 it also be stated

that the current envelope of one phase is having greater distortion compared to the healthy motor. In addition to that Figure 3.11 shows slight speed fluctuation when it has reached to steady state condition.

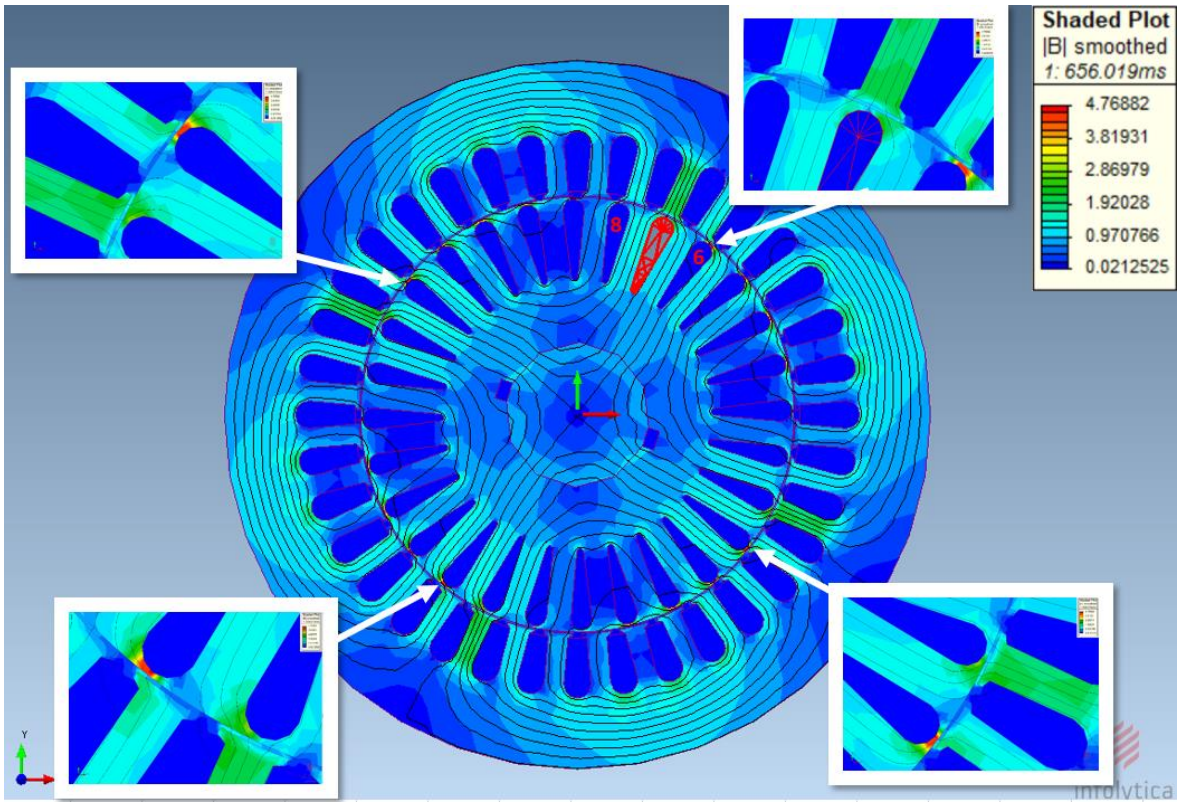

Figure 3.4. One broken bar (656ms)

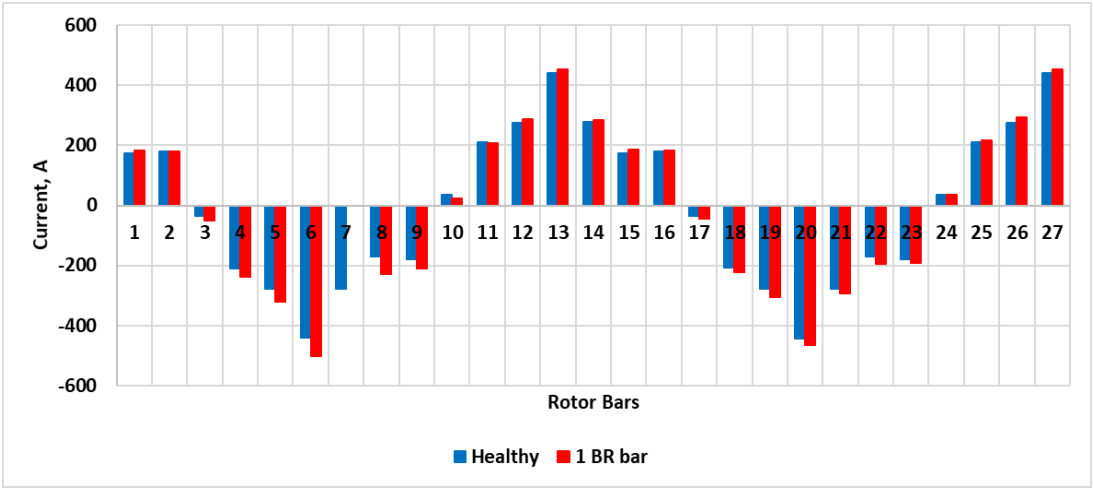

Figure 3.5. Current distribution in rotor at 656 ms - one broken bar

On Figure 3.6, setup with two broken bars is shown, which is very similar to the one broken bar case. Deviations caused by the two broken bars impact behaviour even more and this is highlighted through Figure 3.10 and Figure 3.11. Speed and current envelopes are distorted. In addition to that current distribution between the bars becomes even more disproportionate. As an interesting phenomenon on Figure 3.5, all the currents with negative polarity have significant amplitude value increase compared to the healthy motor.

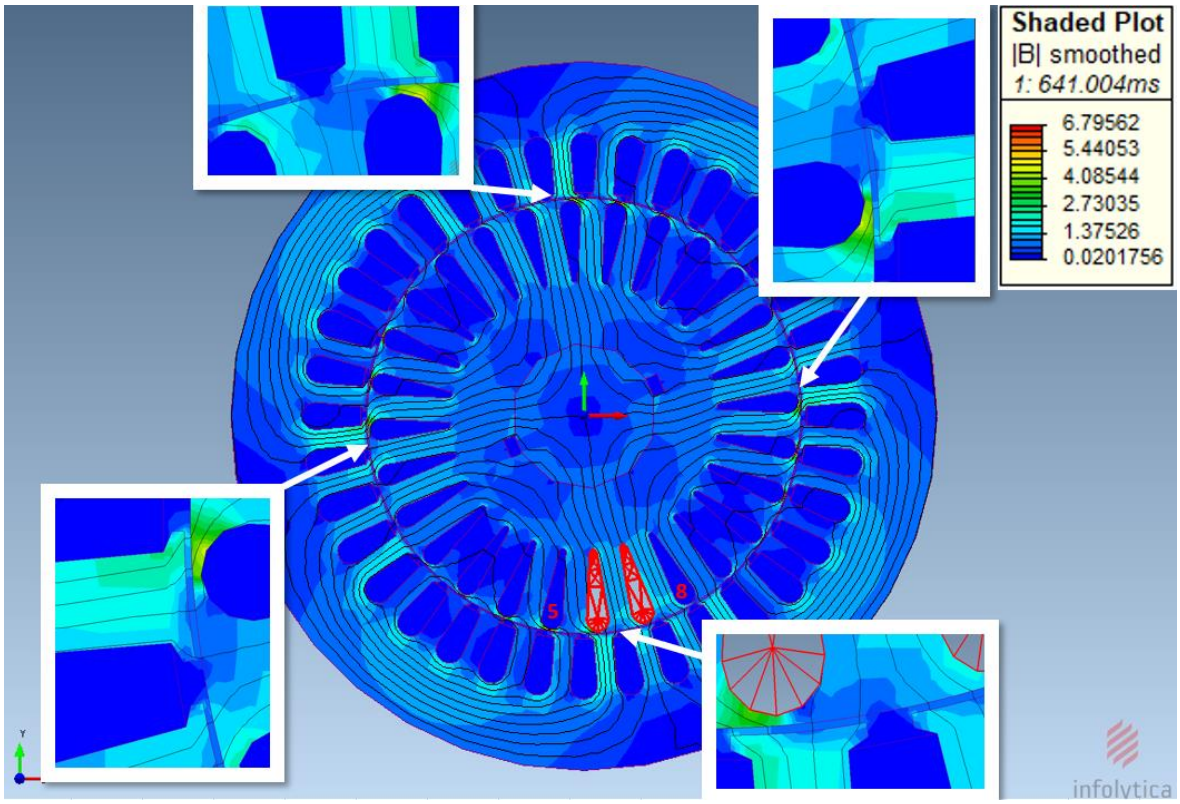

Figure 3.6. Two broken bars (641ms)

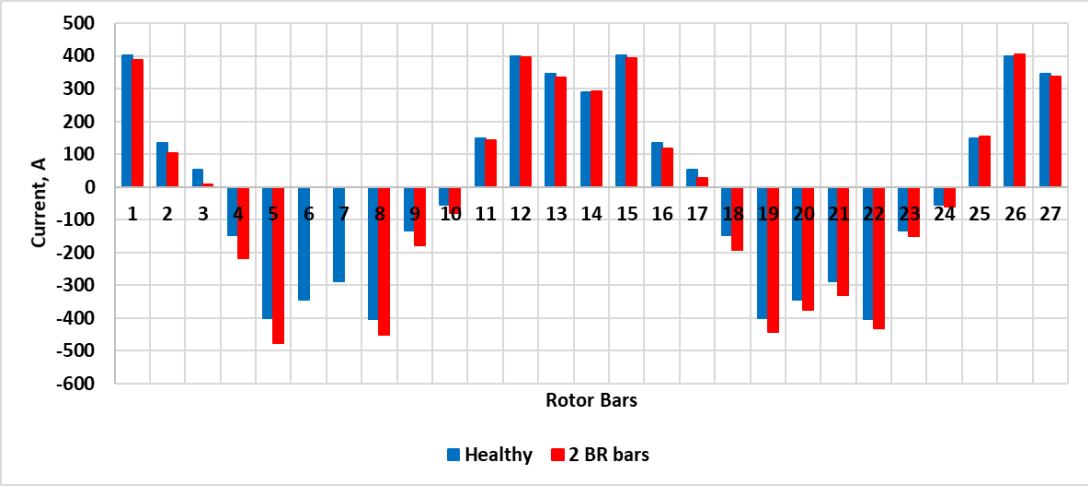

Figure 3.7. Current distribution in rotor at 641 ms - two broken bars

Out from all the broken bar faults, Figure 3.8 highlights most adequately the induction motor behaviour when the fault with three bars occurs. As shown on that figure, magnetic flux distribution in the rotor is greatly affected. Secondly, rotor bar 8 current on Figure 3.8 has made a two-fold increase compared to the healthy motor. When referring to Figure 3.10 and Figure 3.11 it can be seen that the deviations have increased even further.

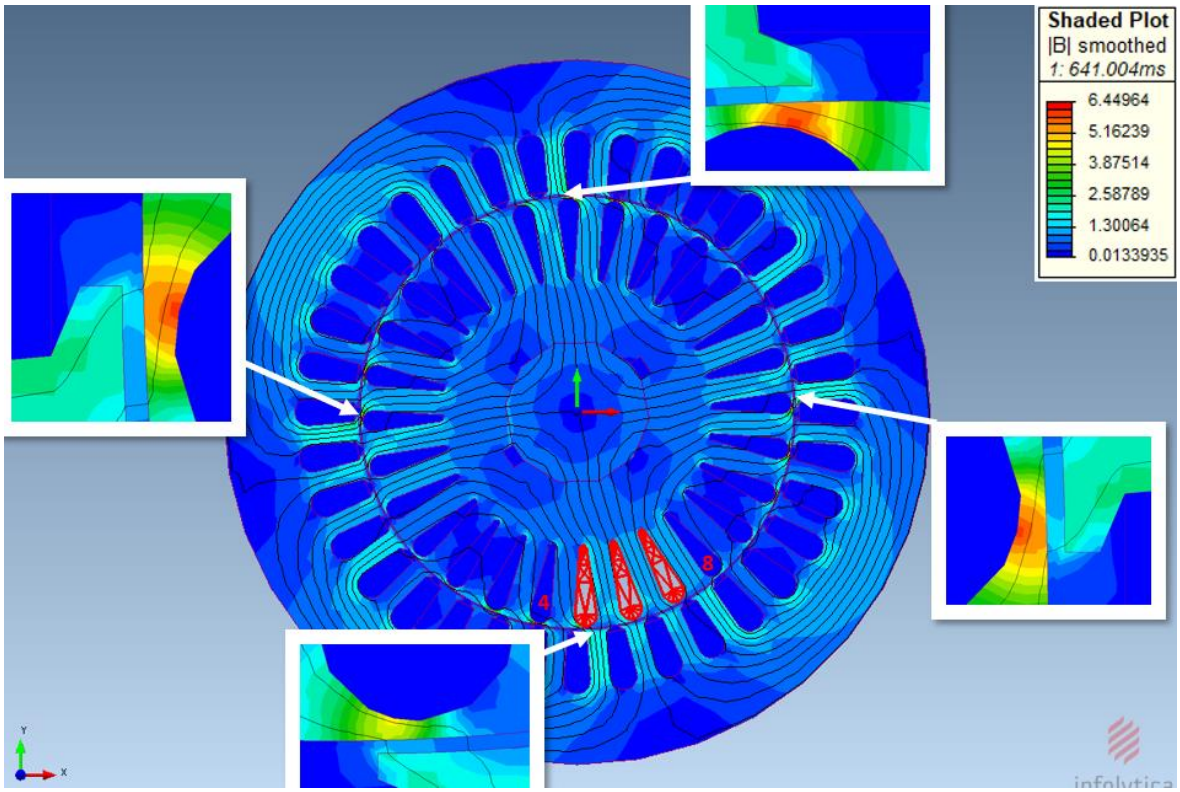

Figure 3.8. Three broken bars (641 ms)

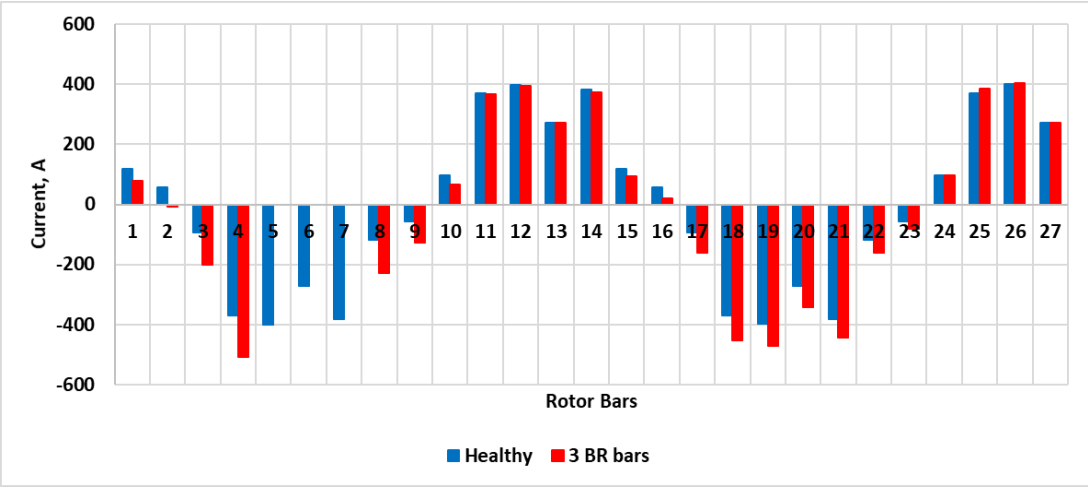

Figure 3.9. Current distribution in rotor - three broken bars (641ms)

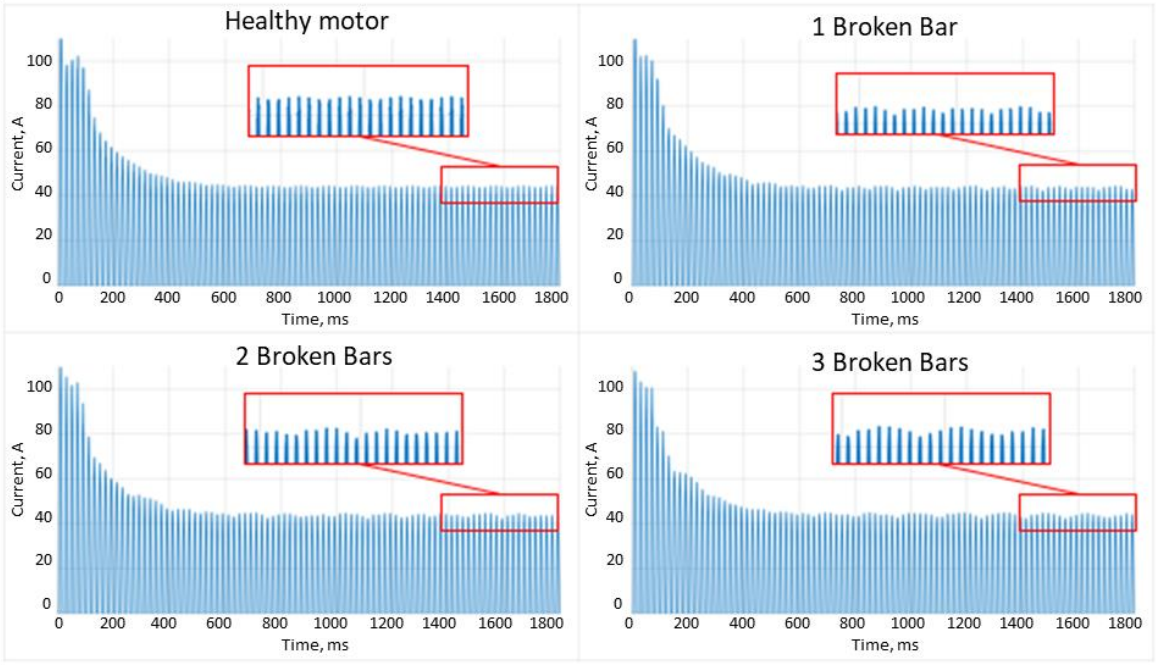

Figure 3.10. Positive half of current envelope from stator - healthy and broken bars

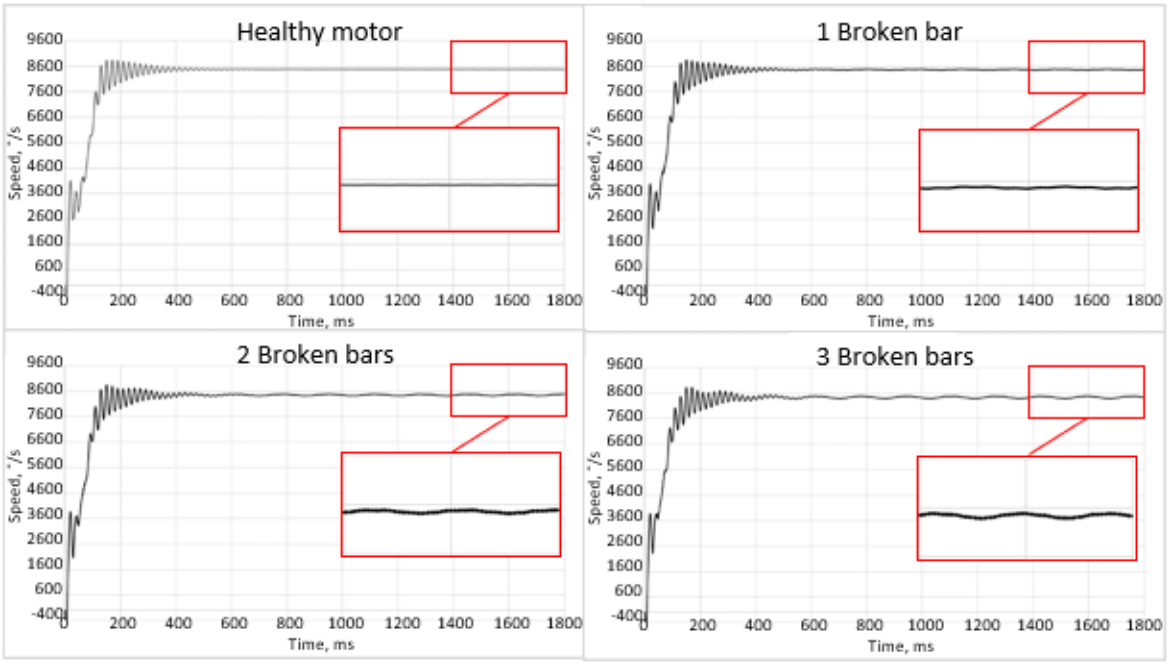

Figure 3.11. Speed of induction motor under healthy condition and broken bars

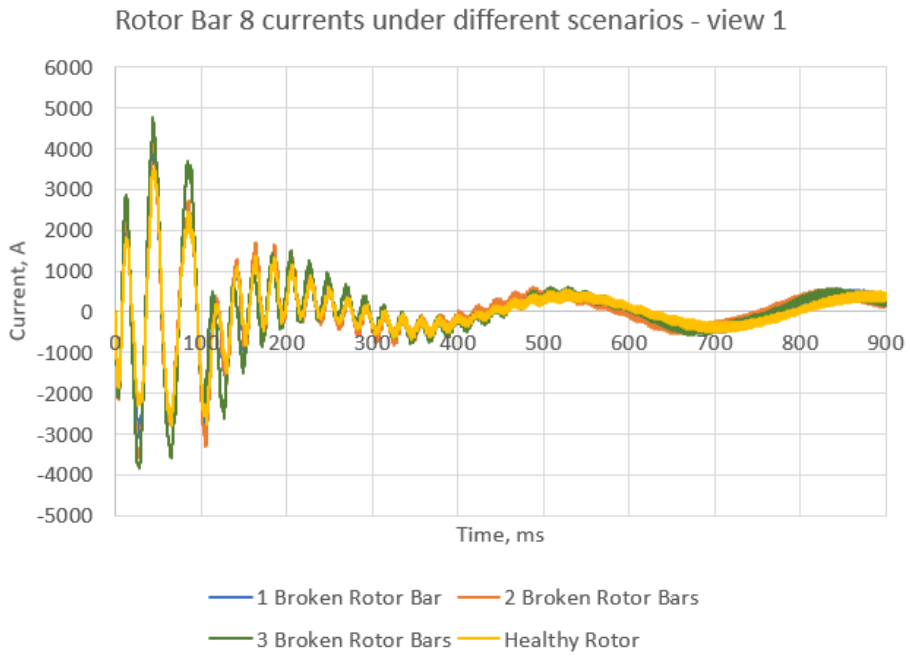

Figure 3.12. Rotor bar 8 current from start-up till steady state condition

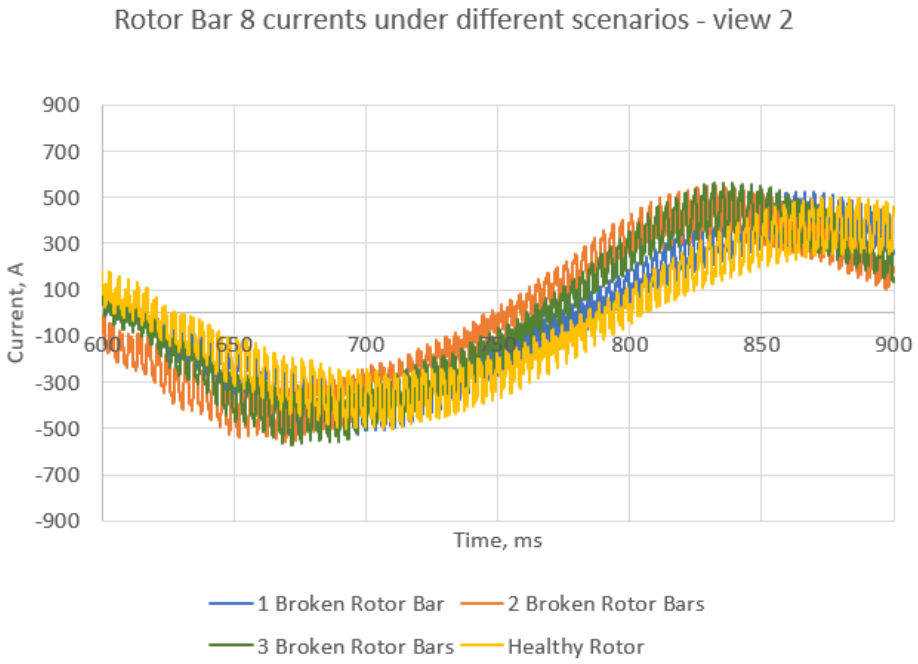

Figure 3.13. Close view of rotor bar 8 current in steady state

On Figure 3.12 and Figure 3.13 rotor bar 8 currents are shown under different scenarios. There are several conclusions, which can be drawn out. Firstly, when the quantity of adjacent broken motor bars increment, the current amplitude of the adjacent healthy bar increases. Secondly, the current waveform of the healthy motor stays ahead of the broken rotor bar motors. Thus, from the rotational speed perspective, faulty machine lags behind healthy machine.

On Figure 3.14, the frequency spectrum of simulation data is shown. Different patterns start emerging from this figure. For example, on the healthy machine there are no significant frequency spectrum distortions close to first (50Hz) and third (150Hz) harmonics. However, if there are broken bars, then these harmonics come imminent and start evolving unique patterns. In the three broken bars case, there are significant distortions close to 50, 150 and 250 Hz. Shoulders close to 50 Hz are unique to rotor bar faults.

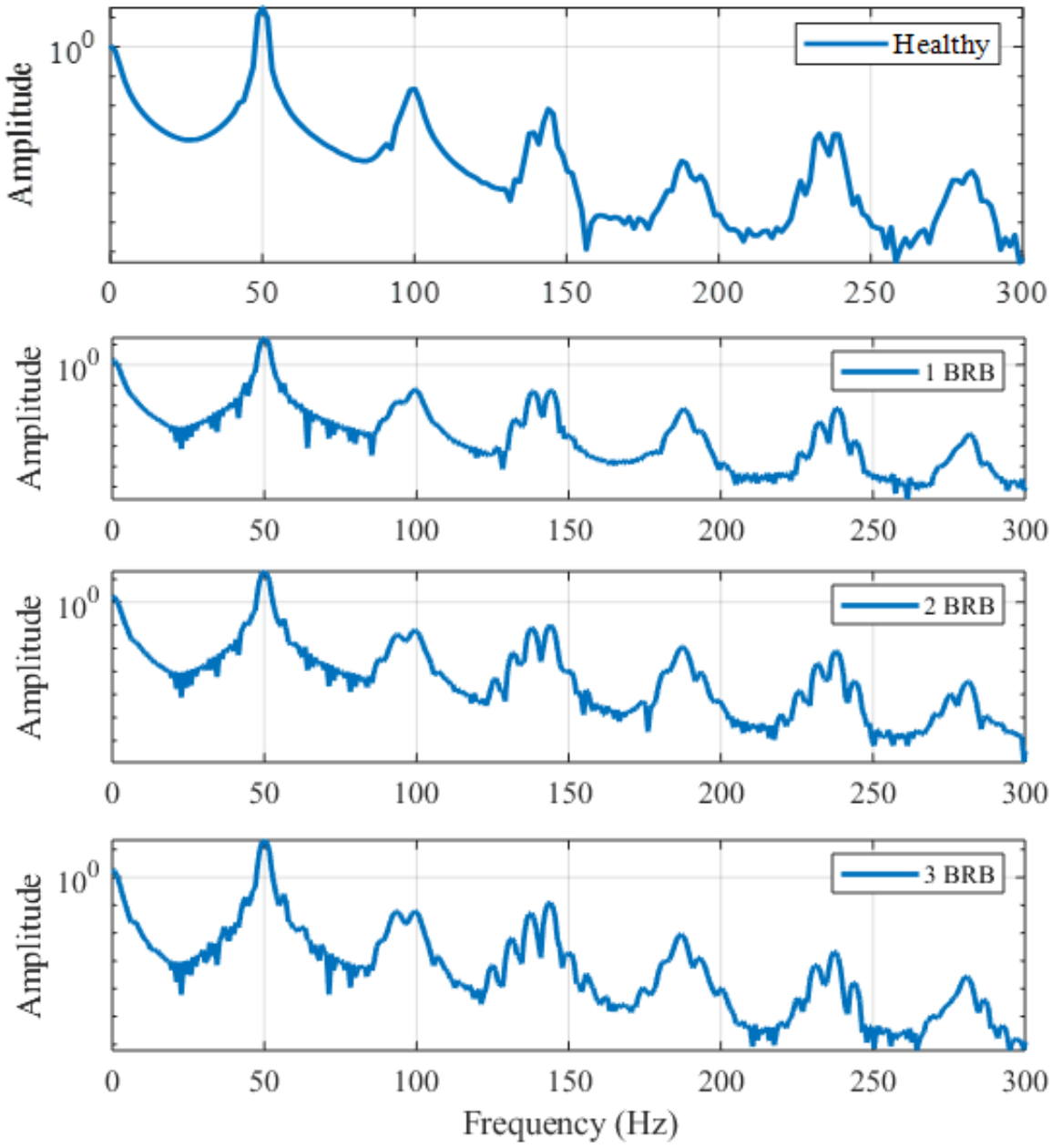

Figure 3.14. Simulation data frequency spectrum

3.2.2 Coil to Coil Fault

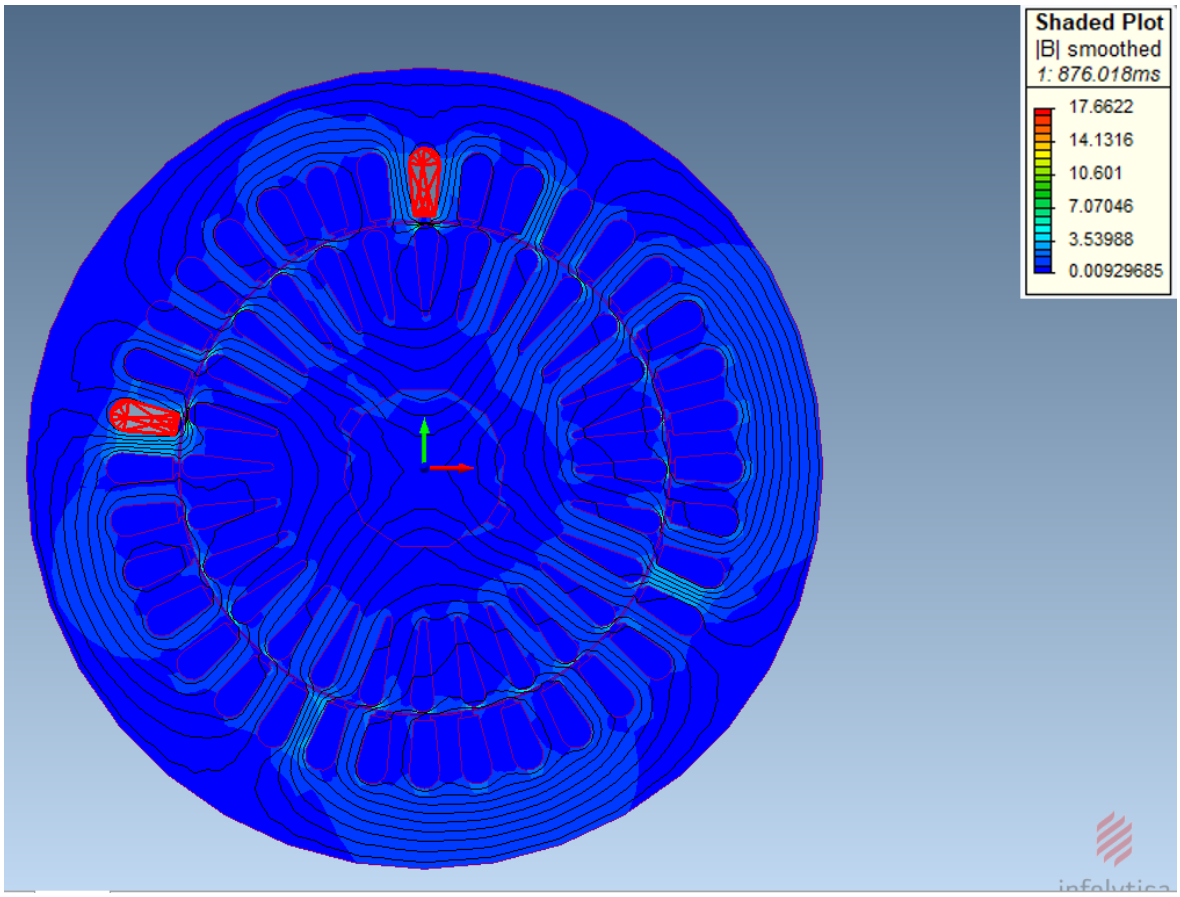

Figure 3.15. Coil to coil fault (876 ms)

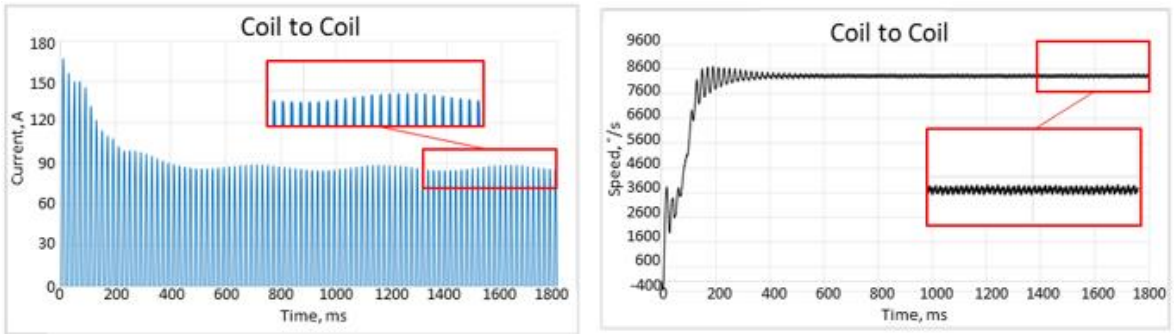

Figure 3.16. Current envelope of the stator (left) and speed of the motor (right)

Coil to coil fault affects cardinally the generation of rotating magnetic fields. As shown on Figure 3.15, the magnetic poles are not uniformly generated and therefore the machine is operating with a lot of disturbances (Figure 3.16, speed). Although wavy current envelope is shown on Figure 3.16 there is another important factor related to it. This is a phase where coil to coil fault occurred. Other phases have significantly lower current amplitude (close to 40 A) than this one. This is a severe fault, which on a practical machine could lead to a fatal breakdown.

3.2.3 Faulty Internal Coil to Coil Connection

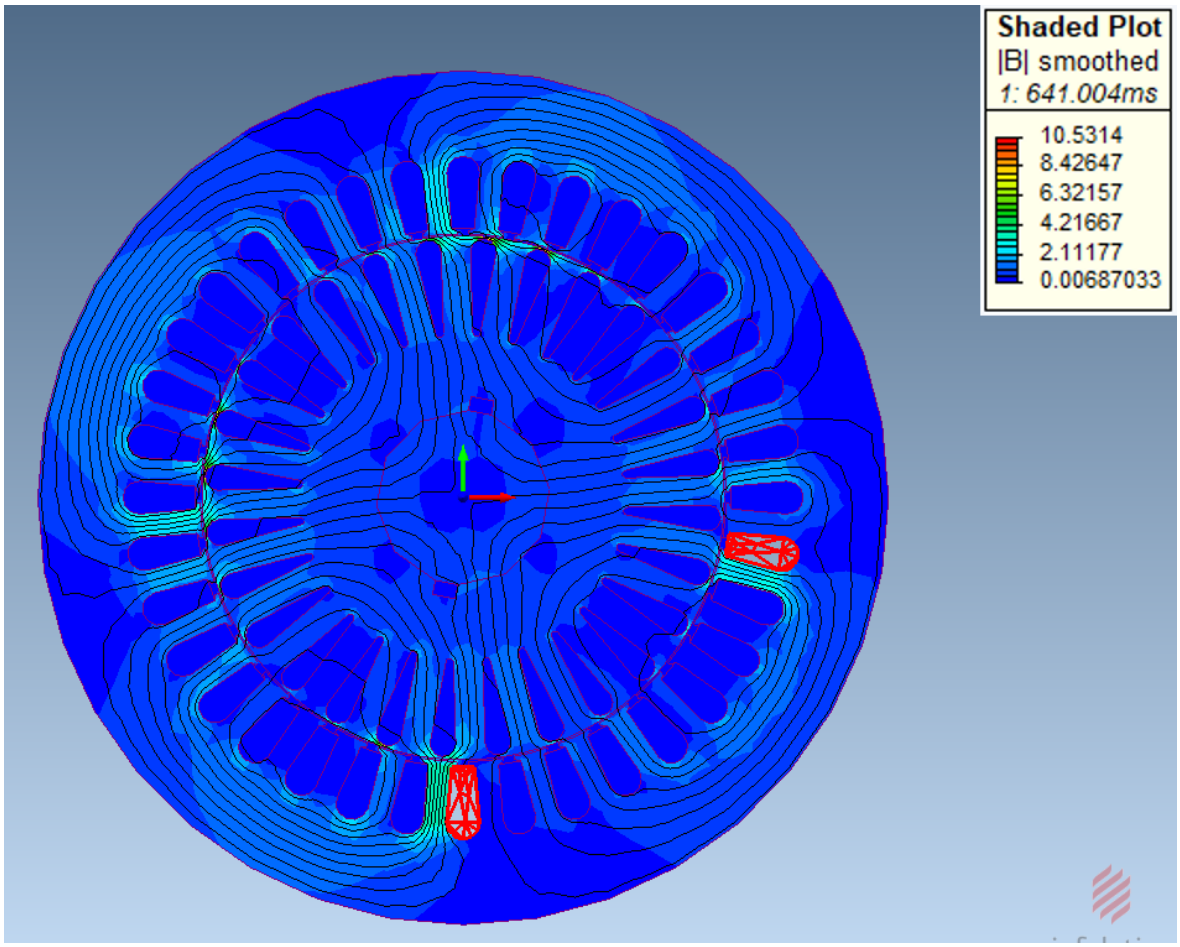

Figure 3.17. Faulty Internal Coil to Coil Connection

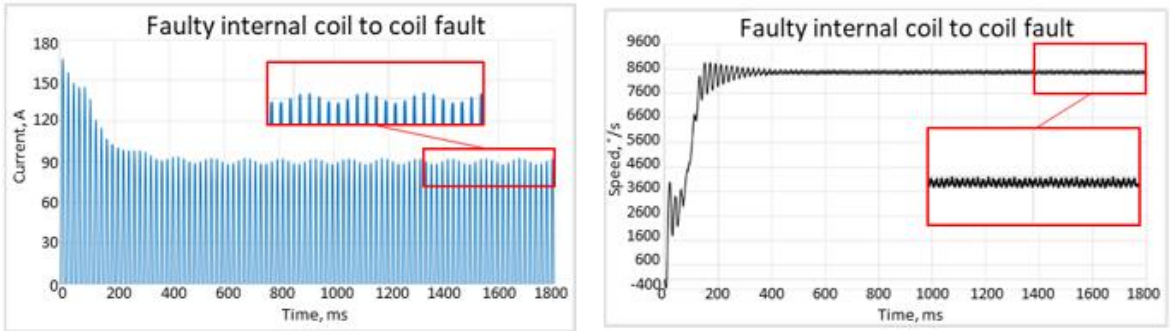

Figure 3.18. Current envelope of the stator (left) and speed of the motor (right)

Faulty internal coil to coil connection has similar effect to the motor as coil to coil fault. Despite of the few differences. For example, the current envelope is more distorted, but the speed of the rotor is higher (Figure 3.18).

4 EXPERIMENTS WITH FAULTY INDUCTION MACHINE

4.1 Experimental Setup

The experimental setup is made up from seven main components. As shown on Figure 4.1, it consists of following objects:

1. ABB ACS800 frequency converter
2. Load motor
3. Induction motor under test (test machine)
4. Analysis device (Dewetron DEWE2-M18)
5. Circuit breaker
6. Current clamps and supply connection box
7. Torque sensor

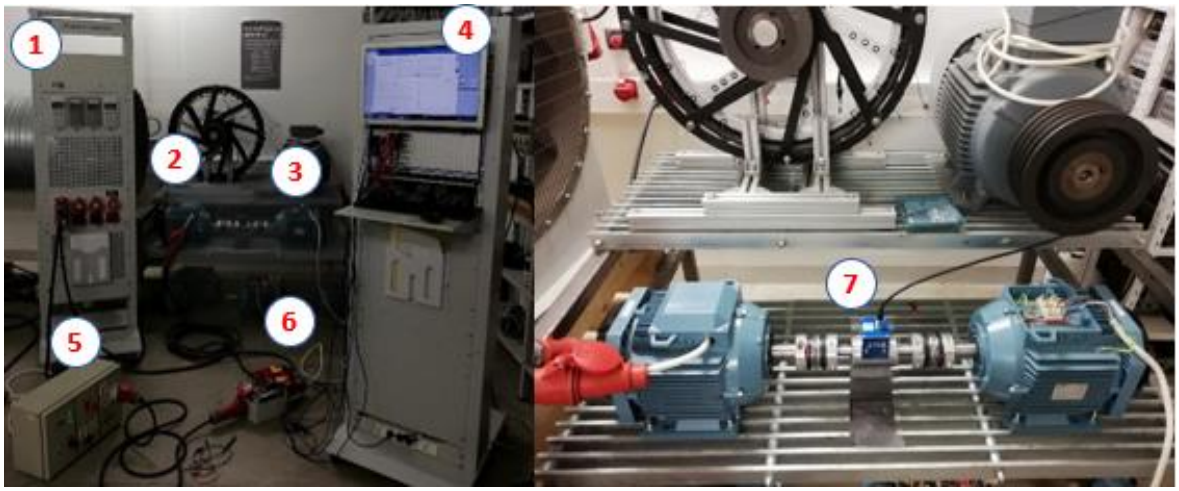

Figure 4.1. Experimental setup

In this setup, the load motor and the test machine are identical. There are only two differences between these motors. As illustrated on Figure 4.2, the load motor is supplied by ACS800 frequency converter and is in star connection. On the other hand, the test machine is directly connected to the grid and is in delta connection. Frequency controller allows effectively control the load motor torque value through DTC mode. 30% is equal to 14.7 Nm and 50% is equal to 24.5 Nm, which is applied to the machine under test. The test machine is connected directly to grid. Direct connection to the grid enables to avoid undesired harmonics coming into the machine spectra. The noise caused by the switching operations in inverter modules would leave a lot of distortions in the frequency spectrum of the test machine. Thus, data becomes more complex and is harder to analyse, if done vice versa. When the drive train is operating, three levels of torque are applied to

test machine – 0, 30, and 50 %. That gives a precise feedback on the machine behaviour under different conditions.

During the operation, the machine is constantly monitored through the torque sensor, current clamps, and voltage probes. Direct values from the sensors are sent as analog or digital signal to the analysis device Dewetron.

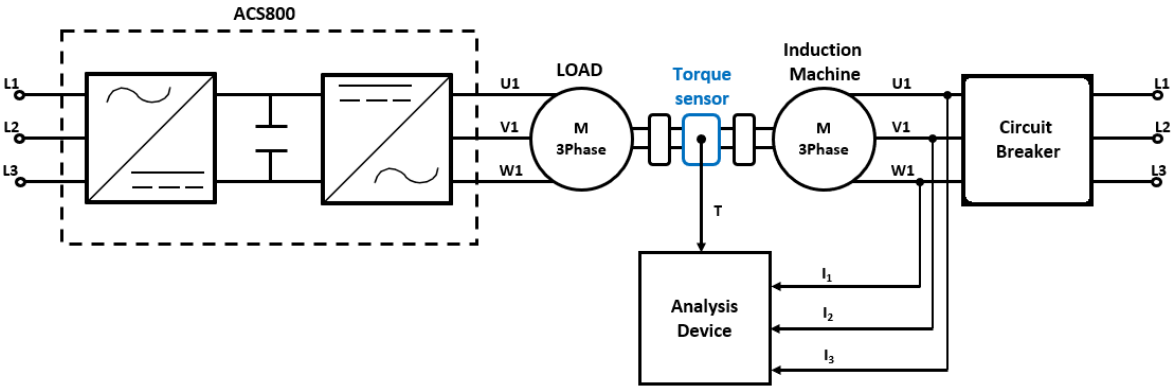

Figure 4.2. Connection diagram

Data recording in the analysis device starts when the machine has reached to the steady state condition. This means, that the transient period (start-up) is finished. After that, the machine is monitored with the sampling time of 6000 ms and sensors data recording is with frequency of 10 kHz. This will generate a huge amount of data, which can be analysed further in Dewetron (spectrum analysis – „Hanning -32 dB“, current envelopes, current signature, etc.) or in MatLab.

In this experimental setup, four types of test machines are used. Firstly, the healthy motor is tested, and all the data is stored in the analysis device. Eventually, this data will serve as a benchmark to all other tests. Thereafter, the test machine gets a new rotor and all the steps are repeated.

Figure 4.3. One broken rotor bar

Three additional measurements are required to be carried out after the healthy one. Tests with setups of one (Figure 4.3), two (Figure 4.4) and three (Figure 4.5) broken rotor bars are done.

Defining the exact location of the rotor bars was difficult as they were skewed. To ease the problem, a reference rotor was taken and cut half. This action was also necessary for designing the rotor in FEM software. Drilled holes are 7 mm in diameter and 26 mm in depth.

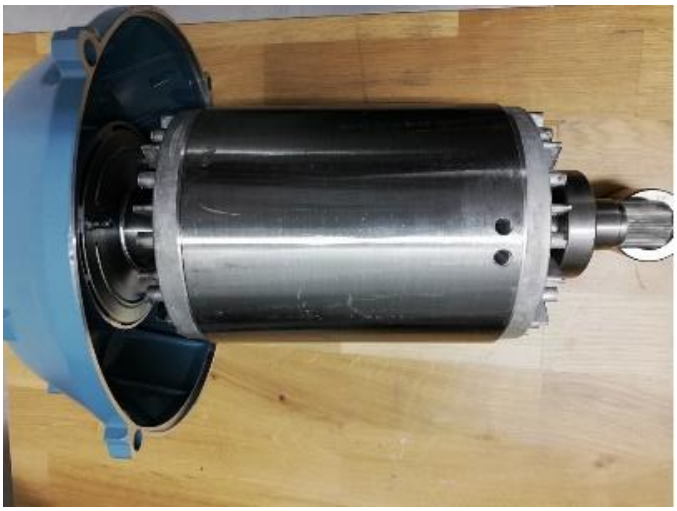

Figure 4.4. Two broken rotor bars

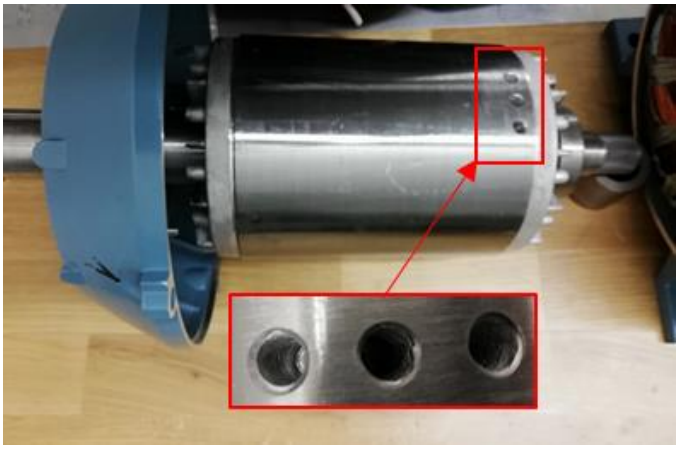

Figure 4.5. Three broken rotor bars

4.2 Experimental Results and Discussion

4.2.1 Healthy motor

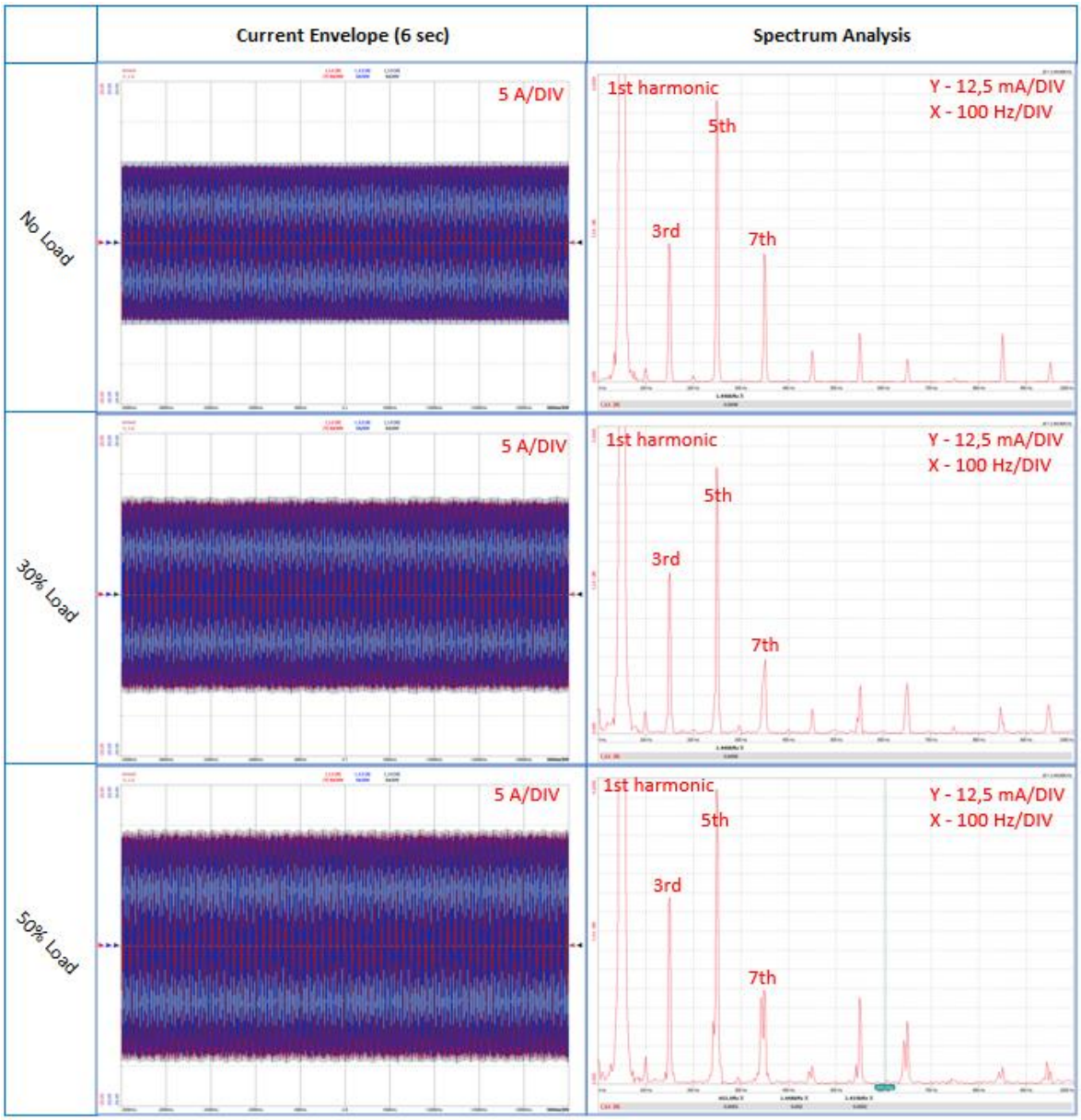

Figure 4.6. Current envelope and spectrum analysis (Hanning -32dB) of healthy motor

From the experimental setup, the healthy motor does not show any variations close to odd harmonics. There is a very firm pattern which stands out. The first harmonic is the strongest component as expected, but the second strongest component is the fifth harmonic and the third harmonic is greater or close to seventh harmonic. On the current envelope side when load is applied, only the increase of current amplitude is visible and envelope remains smooth.

4.2.2 Broken Rotor Bars

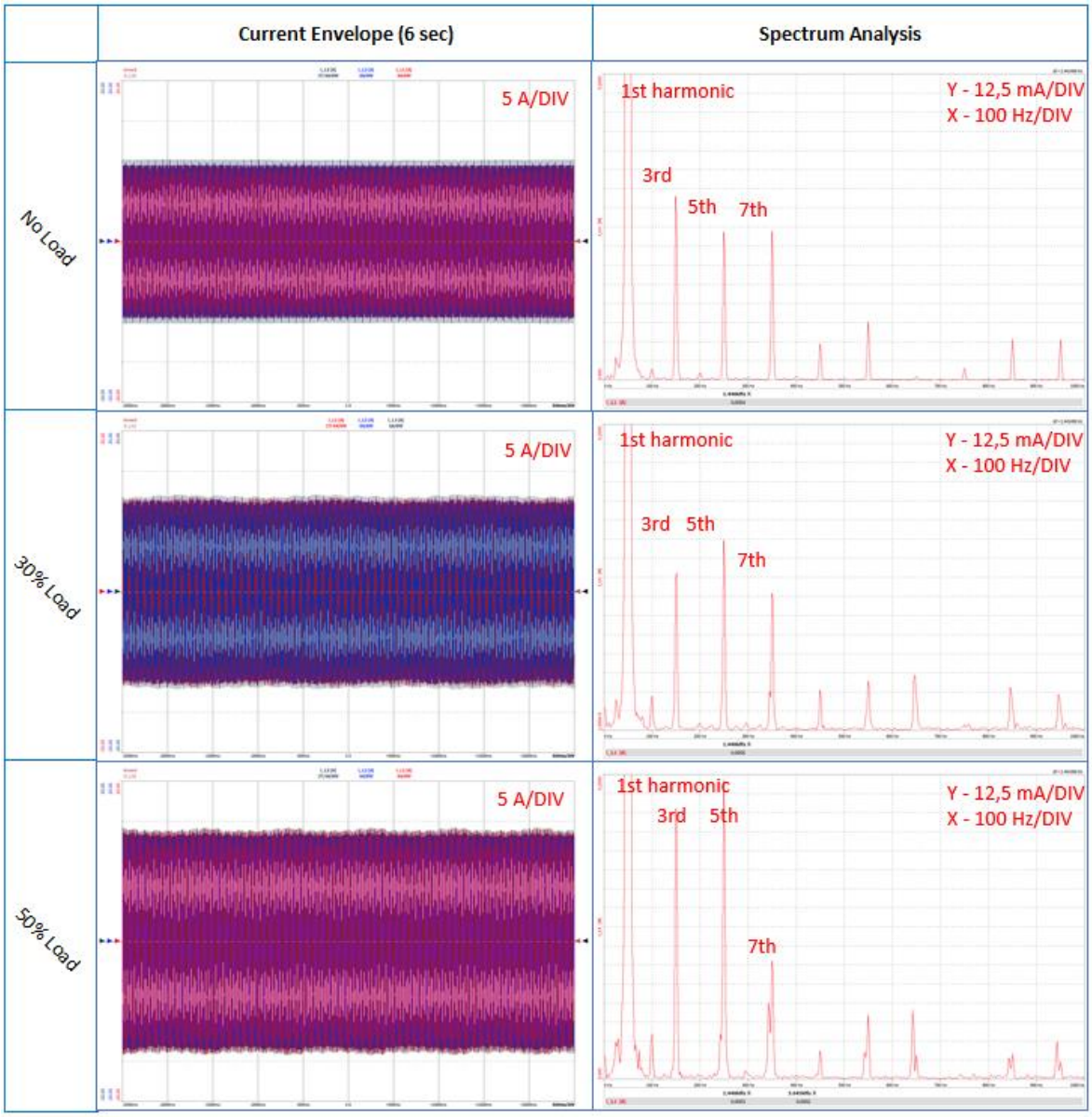

Figure 4.7. Current envelope and spectrum analysis (Hanning -32dB) of 1 broken bar

On the Figure 4.7 significant distortions start appearing close to the first harmonic when the load is applied to the test machine. In addition to the first harmonic, when the load is close to 30% distortions appear near the fifth harmonic. As compared to the healthy motor, there is no firm pattern detectable between the main harmonics or with the current envelopes, as they start randomly changing positions on the magnitude side.

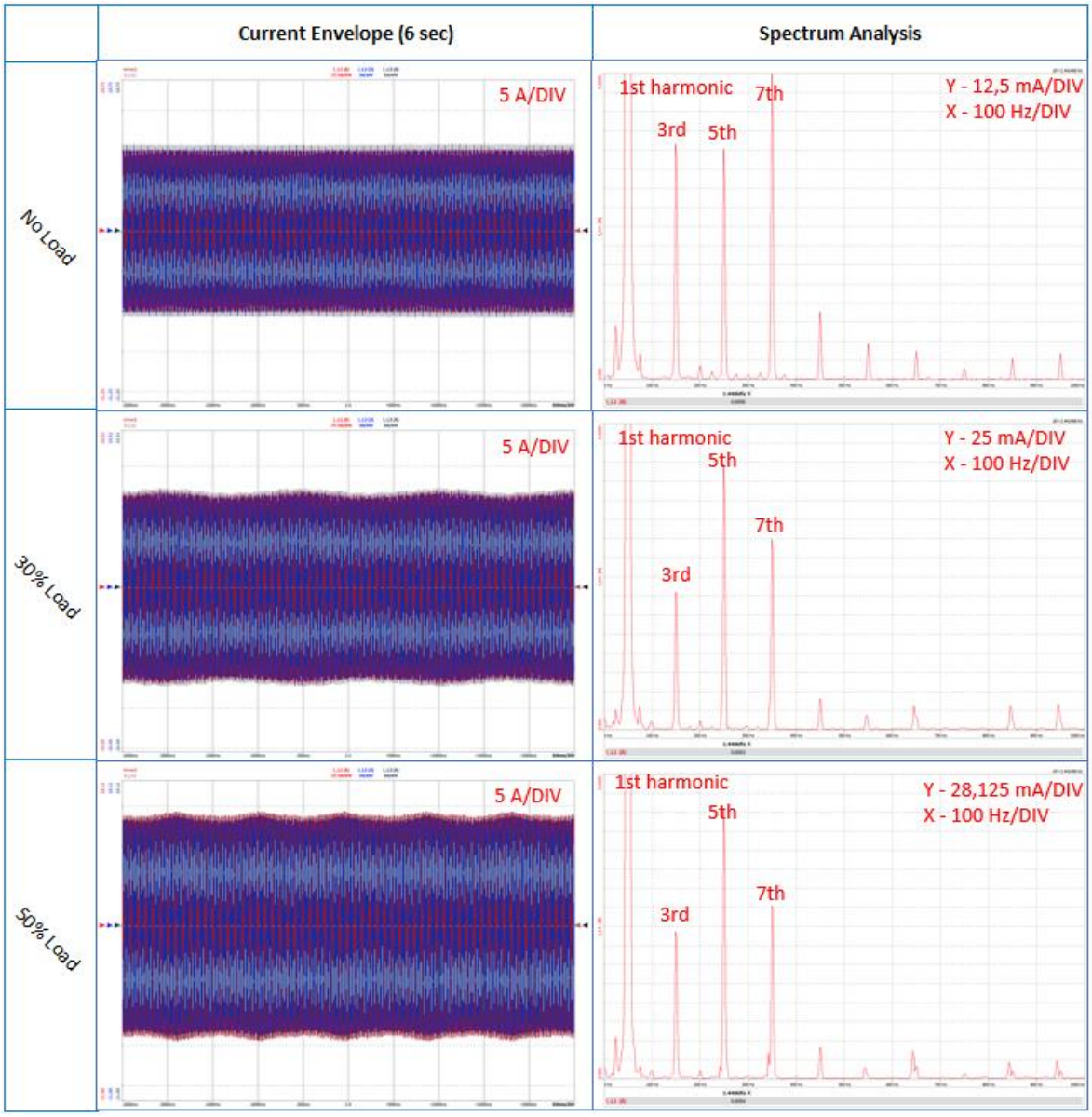

Figure 4.8. Current envelope and spectrum analysis (Hanning -32dB) of 2 broken bars

Two broken bar fault causes significant distortions in the current envelopes and within the frequency spectrum. In general, it is visible already without a load that the amplitudes of third, fifth and seventh harmonic have increased a lot. When the load of 30 or 50% is applied, fifth harmonic is increased twofold. The shoulder pattern close to the first harmonic is verifiable more precisely as rotor bar fault. Furthermore, the current envelope is very unstable. This is a clear indication that the motor is having a serious fault in its operation.

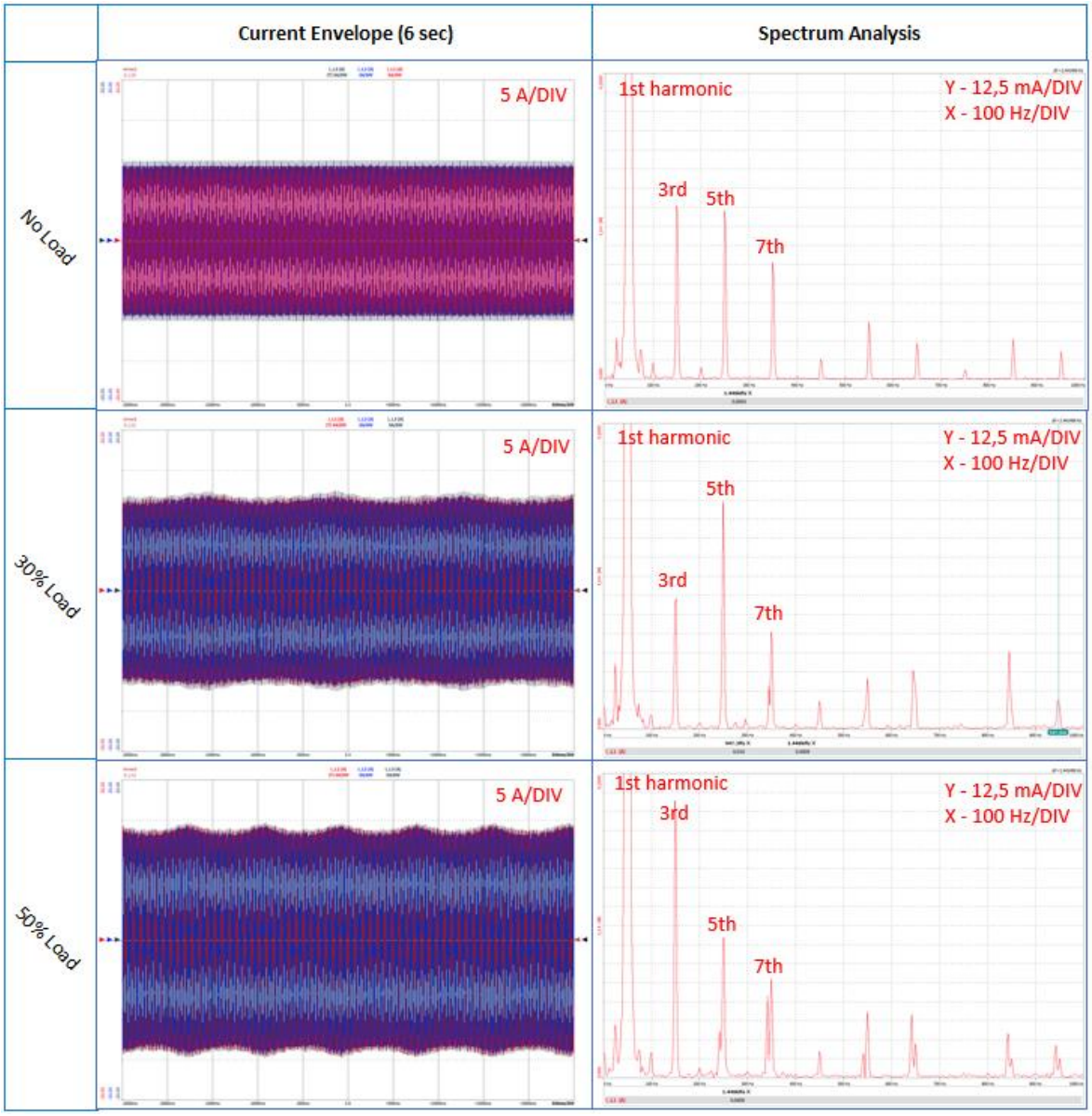

Figure 4.9. Current envelope and spectrum analysis (Hanning -32dB) of 3 broken bars

Induction motor fault with three broken bars is not generating high amplitude levels on the third, fifth, and seventh harmonic. It is also noticeable that with different loads, the previously mentioned harmonics change a lot in comparison of amplitude towards each other. In addition to that, odd harmonics – first, fifth, and seventh - have significant disturbances on sides, when load is applied. Likewise, the current envelope is very unstable when the load is applied.

4.2.3 Torques of Broken Rotor Bars and Healthy Motor

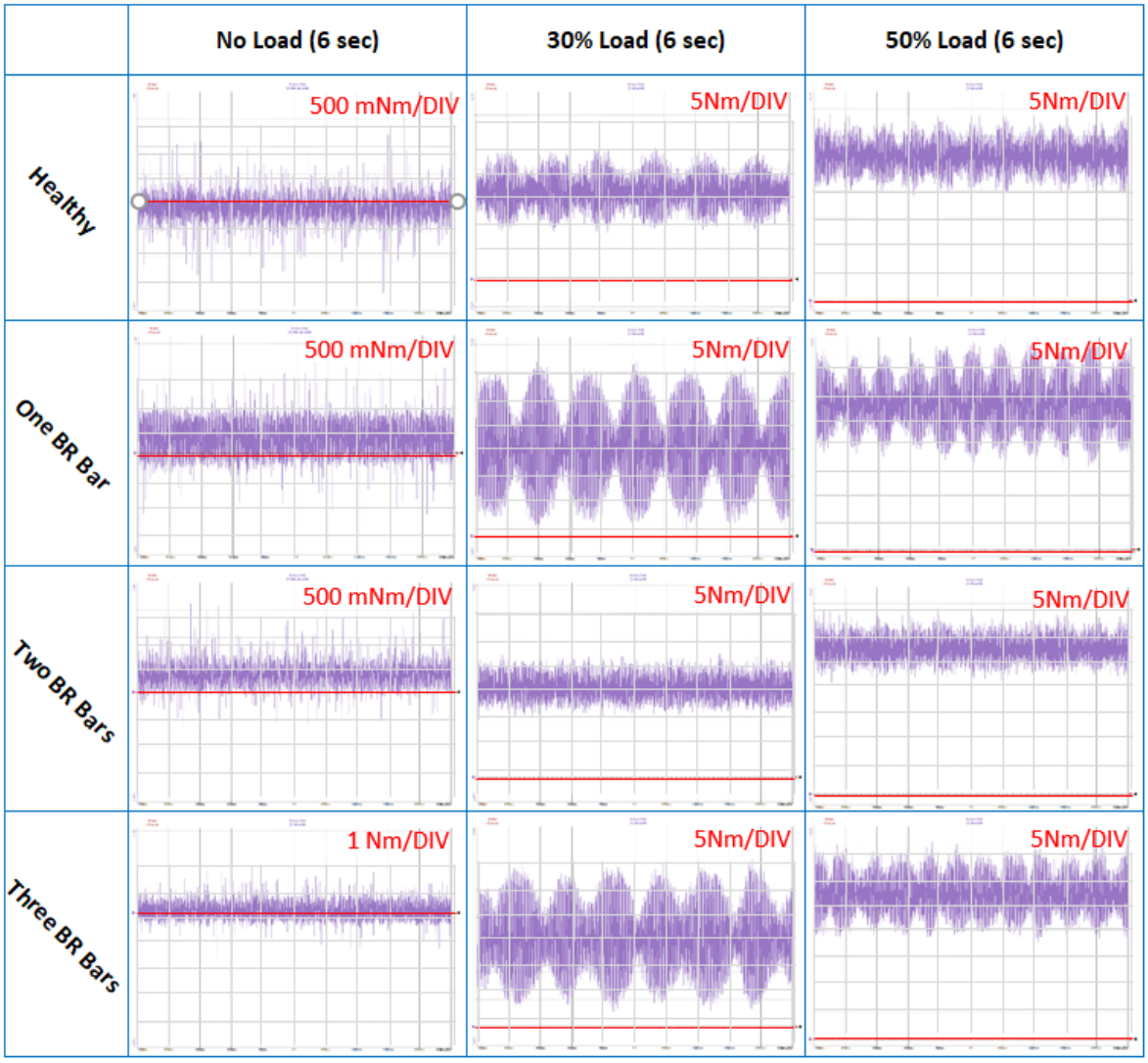

Figure 4.10. Torque values of different setups

As mentioned in Paragraph 4.1, the applied load to line-fed test machine was made via frequency converter, which was operating in DTC mode. Loading motor and test machine were with the same motor parameters.

On Figure 4.10 torque values of different setups are shown. In principle, when no load is applied there are no significant patterns fed back from the drive train by torque sensor. There was only one exception in running the tests. On one broken bar machine significant distortion can be seen when no load is applied. This is caused by the operating frequency converter. It was just powered up and there was no current passing through the loading machine. One the case of two broken bars and healthy motor, frequency converter was completely shut off and no significant distortions from outside environment were coming into the torque sensor.

Things get interesting when the load of the machine is increased to 30%. In comparison to the healthy machine, two broken bar machine does not look similar at all. This test was made for several times, whereas even new torque sensor was used. Despite of these efforts, picture of the torque remained the same. Thus, it must be the actual behaviour of the machine with two broken rotor bars. Furthermore, with one and three broken bar motor tests show the torque ripple increase in the size of amplitude. It is incremented more in one rotor bar than the three broken rotor bars. When load is increased up to 50% of the nominal load, the torque ripples decrease, pattern of the torque gets denser and narrower.

5 SUMMARY / KOKKUVÕTE

5.1 Summary

In this master's thesis the main objective was to investigate the induction motor model under different conditions for the purpose of diagnostics. Extensive literature research was done and it was decided that this thesis will cover broken rotor bar faults on practical setup and various faults in simulation phase. Therefore, measurements, simulations and experiments were carried out.

The first objective was to investigate the experimental machine as thorough as possible. For this purpose, one induction machine was torn apart in a controlled manner. Rotor was cut in half and stator windings were torn out – meanwhile following the leads. After that measurements were carried through on the stator, stator slots, rotor, rotor bars, and windings. This gave enough information to work with. The results from this activity ended up in motor datasheet and in stator windings connection diagram.

After drafting the datasheet, motor was drawn and designed in a software tool called Infolytica. This software enabled to analyse motor behaviour in a controlled environment via Finite Elements Method analysis. All the objects defined in the software had to be given attributes. For example, the material of the object, conductivity, motional elements, outside boundaries, density of the mesh, electrical circuit, etc. Several case studies were made on the motor. Out of these studies, six of them are represented in this thesis – healthy, one broken bar, two broken bars, three broken bars, coil to coil fault, and faulty internal connection. The design, validation, and running the simulation is a huge part of this thesis. Simulations were done with time period of 900 and 1800 milliseconds with data recording of 25 kHz and 1 kHz respectively. Significant amount of information on the model behaviour was received. Afterwards, current data was exported, and fast Fourier transformation was applied to it. That enabled to visualize the frequency spectrum of simulation model. Obtained results showed correlation between the harmonic distortions and the number of faulty bars.

On the practical setup a testbench was set in place. Experiments were carried out with healthy motor in order to record the correct behaviour of the machine. After that three rotors were modified in a way that they had quantity of broken bars 1,2 and 3 in adjacent way. Motor currents, voltages, torque, etc. were recorded with Dewetron analysis device on a 10 kHz rate. Thereafter, these recordings were used to plot the graphs and analyse the frequency spectrum of the machine. The obtained results showed that frequency spectrum changed significantly when different setups were used.

Results obtained from the simulation and experiments are satisfactory. As the author of this thesis I believe that the simulation can be improved even further in order to replicate even more precisely the actual motor itself. This would require more extensive investigation into model design.

The objectives of master's thesis were fulfilled with interesting results obtained.

5.2 Kokkuvõte

Antud lõputöös uuriti elektrimootori erinevaid rikkeid. Esmalt uuriti põhjalikult kirjandust ning seejärel teostati mõõtmised simulatsioonis ja katsestendil. Simulatsioonis katsetati läbi erinevaid rikkelisi olukordi ning katsestendil teostati praktilised mõõtmised nii terve mootori kui ka katkiste rootorivarrastega.

Esmalt oli vaja ära teha põhjalik kaardistus katsetatavast mootoritüübist. Uuritavaks objektiks sai üks põlenud mähisega mootor. Selle mootori rootor lõigati pooleks ning mähised eemaldati staatori uuretest. Antud teguviis võimaldas üles täheldada kõik olulised mootoriosad, mida oli vaja simulatsioonis arvesse võtta. Hiljem oli pooleks lõigatud rootorit võimalik kasutada referentsina katkiste rootorivarraste tekitamisel. Mõõtmistel saadud tulemused on kirjeldatud mootori andmelehel ning staatori mähisejoonisel.

Pärast andmelehe ja mähiste üleskirjeldamist oli võimalik joonestada mootori mudel simulatsioonitarkvarasse Infolytica. Antud tarkvara võimaldas simuleerida ja analüüsida joonestatud mootorimudelit, kasutades selleks lõplike elementide meetodit (*Finite Elements Method*) ehk lühidalt FEM. Kasutatud mudelite puhul oli oluline ära defineerida objektide – staator, rootor, rootorivardad, mähised, jms. – materjalitüübid ning omadused. Katsetati läbi mitmeid erinevaid mudeleid, millest kuus (erinevad mähisevead ja katkised rootorivardad ning terve mootor) on kajastatud käesolevas lõputöös. Simulatsioonid on teostatud ajaseeriaga 900 ms ja 1800 ms, mõõtmistäpsustega vastavalt 25 kHz ja 1 kHz. Saadud mõõtetulemused võimaldasid hilisemalt uurida lähemalt ka sagedusspektrumit. Sealt nähtus, et rootorivarraste järk-järguline purumine mõjutab tunduvalt mootori voolus esinevaid paarituid harmoonilisi.

Praktilises osas sai sooritatud terve ja katkiste rootorivarrastega mootri mõõtmised. Sealt nähtus samuti, et paaritud harmoonilised said tunduvalt mõjutada ning näiteks esimese harmoonilise lähedusse tekkisid niiöelda õlad, mis on väga äratuntav muster katkiste rootorivarraste puhul. Mõõtmised viidi läbi 10 kHz mõõtetäpsusega.

Autori seisukohast vaadatuna saab kindlasti antud mudelit täiustada, selleks et saada veelgi täpsem jäljend tegeliku mootoriga.

Antud lõputöö puhul said põhilised eesmärgid täidetud ning seega võib lugeda seda edukaks.

LIST OF REFERENCES

[1] I. Boldea and S. A. Nasar, The Induction Machine Handbook, Boca Raton: CRC Press LLC, 2002, pp. 2-4.

[2] "ABB Motors - ABB Distributor - Trielectric Internationa FZE," Trielectric Internationa FZE, 22 May 2019. [Online].

Available: http://www.motorsandgenerators.com/Home/Spare_Parts_for_Motors.

[3] N. N. Mansurov and V. Popov, Teoreetiline Elektrotehnika, Tallinn: Kirjastus "Eesti Raamat", 1965, pp. 531-535.

[4] Danfoss Corporation, Handbook | VLT® Frequency Converters - Facts Worth Knowing About Frequency Converters, PE-MSMBM/ColorSigns, 2014, pp. 19-21.

[5] H. Puurand, Üldelektrotehnika, Tallinn: Kirjastus: "Valgus", 1996, p. 194.

[6] Tallinna Tööstushariduskeskus, "Täiturid," [Online]. Available: https://www.tthk.ee/MEH/Taiturid_5.html. [Accessed 23 April 2019].

[7] General Electric Company, "Motor Protection Principles," [Online]. Available: https://www.gegridsolutions.com/multilin/family/motors/principles.htm. [Accessed 23 April 2019].

[8] N. Bianchi, Electrical Machine Analysis Using Finite Elements, Boca Raton: CRC Press, 2005, pp. 21-22,25-26.

[9] T. Vaimann, *Diagnostics of Induction Machine Rotor Faults Using Analysis of Stator Signals,* Tallinn: TUT PRESS, 2014, pp. 18,26.

[10] A. Hand, Electric Motor Maintenance and Troubleshooting, New York: McGraw-Hill Companies, Inc, 2001, pp. 289-319.

[11] A. H. Bonnett, "Analysis of Winding Failures in Three-Phase Squirrel Cage Induction Motors," *IEEE TRANSACTIONS ON INDUSTRY APPLICATIONS,* Vols. VOL. IA-14, no. NO. 3, pp. 223-226, 1978.

[12] EASA, “Typical Failures in Three-Phase Stator Windings,” 19 May 2019. [Online]. Available: https://www.easa.com/resources/booklet/typical-failures-three-phase-stator-windings.

[13] A. H. Bonnet and G. C. Soukup, “Rotor Failures in Squirrel Cage Induction Motors,” *IEEE TRANSACTIONS ON INDUSTRY APPLICATIONS,* Vols. IA-22, no. NO. 6, pp. 1165-1172, 1986.

[14] S. Bachir, S. Tnani, J.-C. Trigeassou and G. Champenois, “Diagnosis by Parameter Estimation of Stator and Rotor Faults Occurring in Induction Machines,” *IEEE TRANSACTIONS ON INDUSTRIAL ELECTRONICS,* vol. 53, no. 3, pp. 963-973, 2006.

[15] I. Y. Onel and M. E. H. Benbouzid, “Induction Motor Bearing Failure Detection and Diagnosis: Park and Concordia Transform Approaches Comparative Study,” *IEEE/ASME TRANSACTIONS ON MECHATRONICS,* vol. 13, no. 2, pp. 257-262, 2008.

[16] A. H. Bonnet, “Cause and analysis of bearing failures in electrical motors,” *Copyright material IEEE, PCIC-92-23,* pp. 87-95, 1992.

[17] B. Asad, T. Vaimann, A. Rassõlkin, A. Kallaste and A. Belahcen, “A Survey of Broken Rotor Bar Fault Diagnostic Methods of Induction Motor,” *Scientific Journal of Riga Technical University,* vol. 14, no. 2, pp. 117-124, 2018.

[18] G. Bergland, “A Guided Tour of Fast Fourier Transform,” *IEEE Spectrum,* vol. 6, pp. 41-52, 1969.

[19] G. Jose and V. Jose, “Induction Motor Fault Diagnosis Methods: A Comparative Study,” *International Conference on Electrical Engineering,* pp. 63-69, 2013.

[20] J. A. Antonino-Daviu, A. Quijano-Lopez, V. Fuster-Roig and C. Nevot, “CASE STORIES OF INDUCTION MOTORS FAULT DIAGNOSIS BASED ON CURRENT ANALYSIS,” in *Petroleum and Chemical Industry Conference Europe (PCIC Europe)*, Valencia, 2016.

[21] J. Cusido, J. Rosero, E. Aldabas, J. A. Ortega and L. Romeral, “New Fault Detection Techniques For Induction Motors,” *Electrical Power Quality and Utilisation,* vol. II, no. 1, pp. 39-46, 2006.

[23] TRIELECTRIC INTERNATIONAL FZE, “Home/Spare_Parts_for_Motors,” [Online]. Available: http://www.motorsandgenerators.com/Home/Spare_Parts_for_Motors. [Accessed 21 April 2019].

[24] M. S. R. Krishna and R. K. S, “Fault Diagnosis of Induction Motor using Motor Current Signature Analysis [ICCPCT-2013],” in *International Conference on Circuits, Power and Computing Technologies*, Nagercoil, 2013.

[25] M. S. R. Krishna and S. H. Kishan, “Neural Network for the Diagnosis of Rotor Broken Faults of Induction Motors Using MCSA,” in *7th International Conference on Intelligent Systems and Control (ISCO)*, Coimbatore, 2013.

APPENDICES

Appendix 1 Stator Winding Diagram

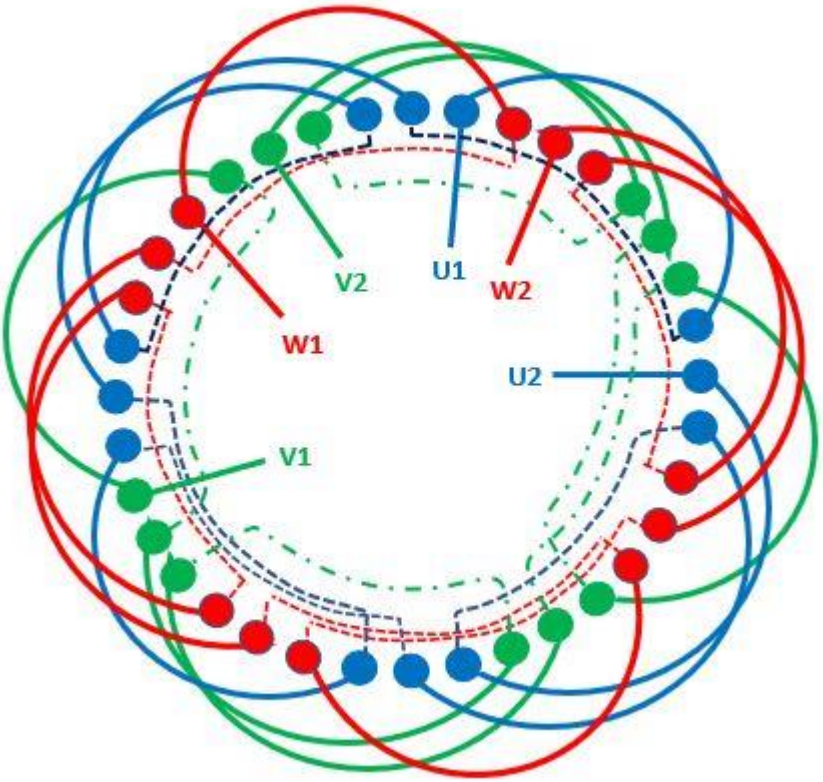

Datasheet: Without number

3	Machine type (cage induction machine)
4	Number of poles
3	Number of phases
1	Number of parallel paths (poles are connected in parallel)
144	Number of conductors in a stator slot
36	Number of turns
4	Number of conductors in turn
1	Number of layers of the stator winding
7/8/8/8/8/7/-||-	Coil pitch in slot pitches (←A/A→/A→; ←B'/←B'/B'→; ...)
50	Frequency of the supply voltage
0.155	Effective length of the machine
0.155	Length of the stator lamination
0.155	Length of the rotor lamination
0.300	Half of the average length of a coil with 7 pitches
0.312	Half of the average length of a coil with 8 pitches
220.0E-03	Outer diameter of the stator core
135.95E-03	Inner diameter of the stator core
36	Number of stator slots
4	Index for the shape of the stator slots
2.0E-03	H1 (see the maps of stator slots)
0.85E-03	H11
0.0	H12
14.30E-03	H13
0.0	H14
0.0	H15
3.0E-03	B11
5.85E-03	B12
8.50E-03	B13
0.0	B14
0.0	B15

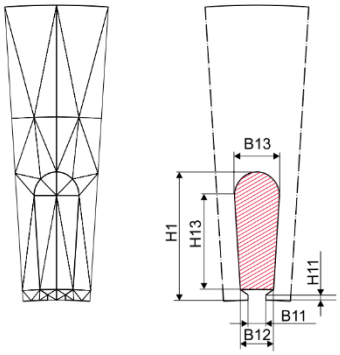

135.0E-03	Outer diameter of the rotor core
45.0E-03	Inner diameter of the rotor core
28	Number of rotor slots
1	Index for the shape of the rotor slots
25.40E-03	H2 (see the maps of rotor slots)
0.50E-03	H21
0.0	H22
21.00E-03	H23
0.0	H24
0.0	H25
0.00E-03	B21
6.75E-03	B22
2.00E-03	B23
0.0	B24
0.0	B25

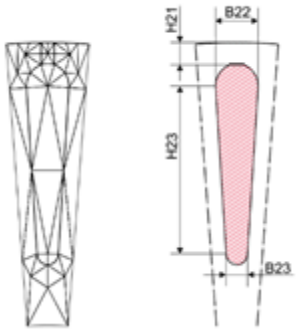

4	Material index for the stator core (BH-curve)
4	Material index for the rotor core (BH-curve)
1	Material index for the rotor shaft (solid nonlinear iron)
0	Material index for the slot wedge (air)
32	Material index for the opening of the rotor slot (Aluminum)

```
11              Material index for the stator coil (Copper)
32              Material index for the rotor bar (Aluminum)

2.2141629e-13   Resistance of a stator phase (ohm)
                End-winding reactance of a stator phase
20.0            Temperature associated with the resistance (C)

375.00E-06      Cross-sectional area of the end-ring
25.00E-03       Radial height of the end-ring
98.00E-03       Average diameter of the end-ring
3.75E-03        Length of the rotor bars outside the core (one end
0.0             Skew of rotor slots in stator slot pitches
```

TABLE I
MAIN PARAMETERS OF THE MACHINE UNDER INVESTIGATIONS

Parameter	**Value**
Number of poles	4
Number of phases	3
Connection	Star/Delta
Number of stator slots	36; non-skewed
Number of rotor slots	28; skewed
Terminal voltage	690V/400V @50 Hz
Rated current	15.3A/8.8A
Rated power	7.5 kW@50 Hz

Healthy Motor

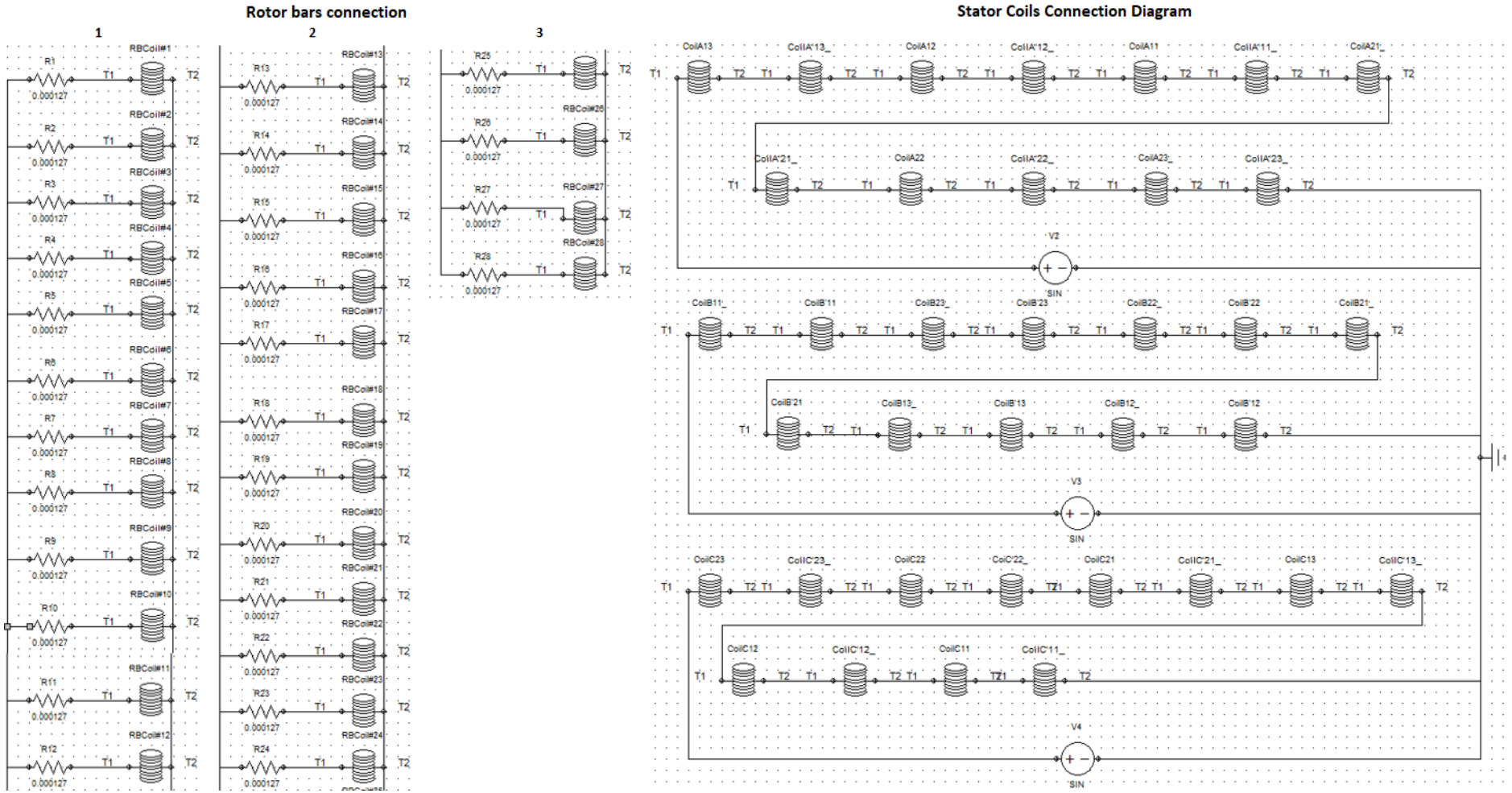

Three Broken Bars

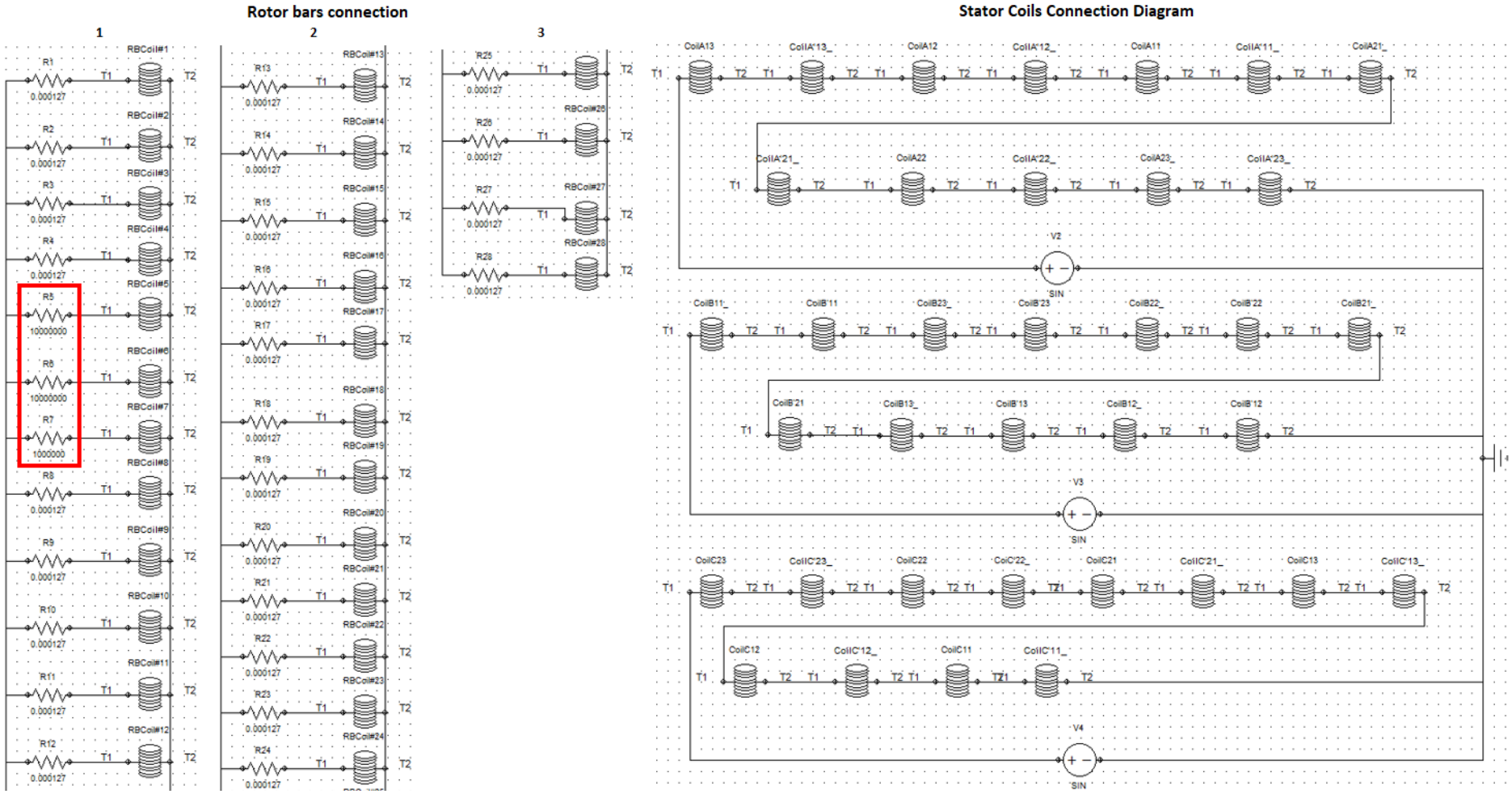

Coil to Coil Fault

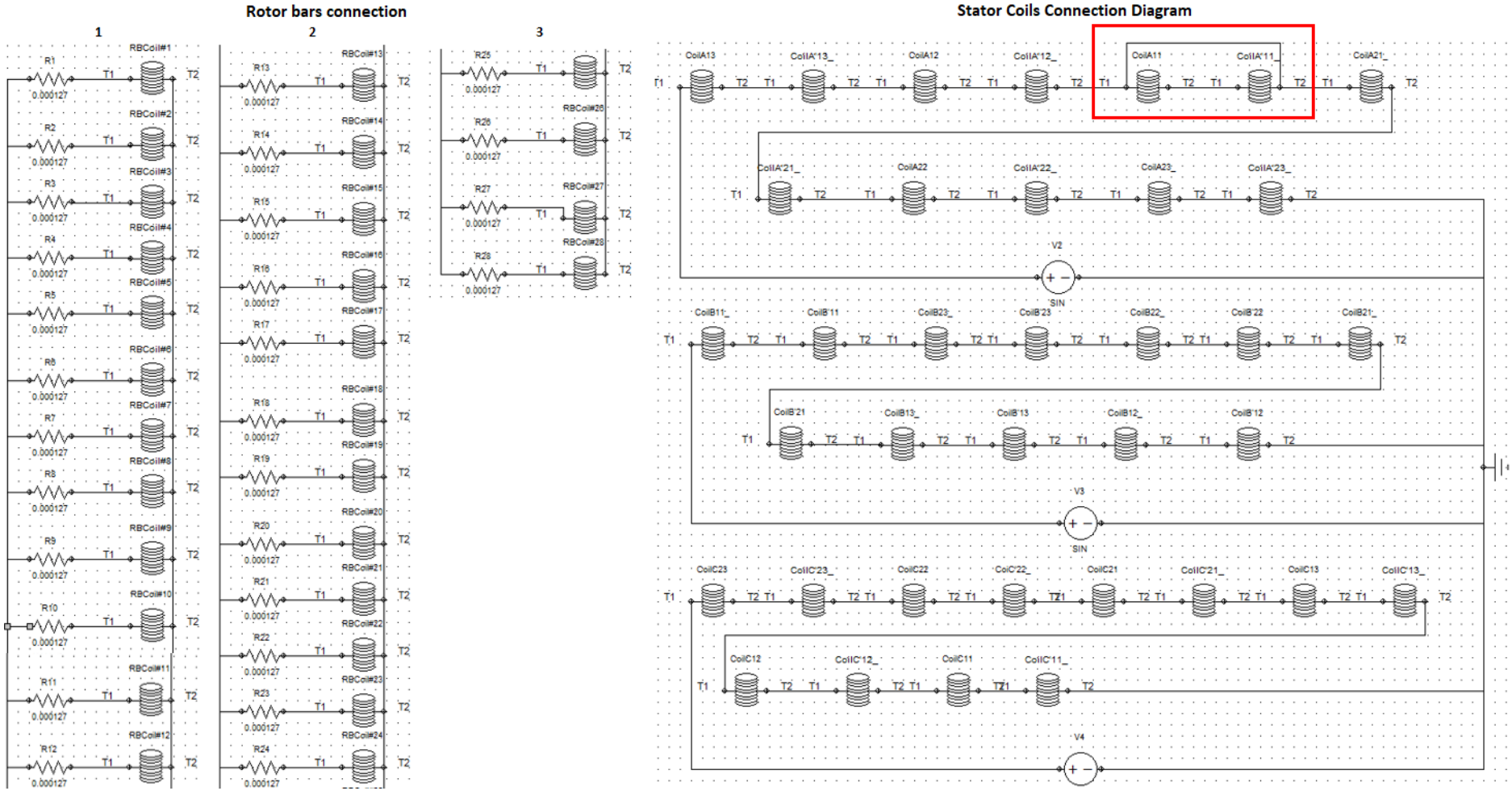

Faulty Internal Coil to Coil Connection